

REFERENCE USE

SLAC-39
UC-28, Particle Accelerators
and High-Voltage Machines
UC-34, Physics
TID-4500 (37th Ed.)

MAGNETIC FIELD MEASUREMENT AND SPECTROSCOPY IN MULTIPOLE FIELDS

February 1965

by

J. K. Cobb and J. J. Muray

Technical Report

Prepared Under

Contract AT(04-3)-400

for the USAEC

San Francisco Operations Office

Printed in USA. Price \$2.00. Available from the Office of Technical
Services, Department of Commerce, Washington 25, D.C.

TABLE OF CONTENTS

	Page
I. Introduction	1
II. Field distribution in multipoles	1
A. The ideal quadrupole magnet	1
B. Origins of higher poles in quadrupole magnets	7
C. Origins of poles with four-fold symmetry	7
D. Origins of poles with two-fold symmetry	10
E. Origins of asymmetric poles	13
III. Magnetic center location	13
A. Experimental	13
B. Symmetry relations in multipole fields	21
C. Theory of light scattering on aligned particles in multipole fields	26
D. Light scattering on aligned particles in a quadrupole field	29
E. Light scattering on aligned particles in sextupole and octupole fields	31
F. Applications	34
IV. Measurement of the effective length in multipoles	37
V. Spectroscopy of multipoles	41
A. Experimental setup	41
B. Coil design and calibration	47
C. Center location with rotating coil	56
D. Effective length measurement with rotating coil	59
E. Effect of field perturbation in multipole fields	61
VI. Gradient measurement in multipoles	66
VII. Optical properties of multipoles	70

LIST OF FIGURES

	<u>Page</u>
1. (a) Ideal (theoretical) quadrupole	8
(b) Practical quadrupole	8
2. Quadrupole constructed perfectly with hyperbolic poles but poles truncated at points p and q	9
3. Quadrupole constructed with circular approximation to ideal hyperbolic shape	11
4. Octupole perturbation in a quadrupole field generated by geometrical asymmetry	12
5. Octupole perturbation in a quadrupole field generated by geometrical asymmetry	14
6. Dipole and sextupole fields generated by asymmetric perturbation in a quadrupole	15
7. Experimental setup for magnetic center location in quadrupole magnetic field	17
8. Light scattering pattern in a quadrupole magnetic field ($\theta = 90^\circ$)	18
9. Light scattering pattern in a sextupole magnetic field ($\theta = 0$)	19
10. Light scattering pattern in an octupole magnetic field ($\theta = 0$)	20
11. Interrelation of angles γ , θ , and β in a magnetic field with quadrupole symmetry	23
12. Orientation for a magnetic dipole μ in a magnetic field with quadrupole symmetry	27
13. Magnetic center location setup for a quadrupole magnet . .	35
14. Experimental setup for quadrupole alignment	36
15. Detailed photo of magnetic center location	38
16. Rotating coils method of effective length determination .	42
17. Experimental setup for quadrupole effective length measurement	43
18. Rotating coil assembly for effective length measurement .	44
19. Block diagram of harmonic analyzer for multipole magnetic field spectroscopy	48
20. Experimental setup for harmonic analysis in a quadrupole field	49
21. Response curve for the asymmetric flat coil	53
22. Calibrating multipole magnets for rotating coil calibration for quadrupole field spectroscopy	54

	<u>Page</u>
23. Geometry of coil arrangement on rotating asymmetrical coil . .	55
24. Rotating coil configuration used in multipole field spectroscopy	57
25. Amplitude of first harmonic vs displacement off center	58
26. (a) Effect of perturbation on quadrupole spectrum	60
(b) Effect of perturbation on quadrupole spectrum	62
27. (a) Effect of pole face perturbation on a quadrupole spectrum.	63
(b) Effect of pole face perturbation on quadrupole spectrum .	64
(c) Effect of pole face perturbation on quadrupole spectrum .	65
28. Probe arrangement for making gradient measurements in quadrupoles	67
29. System layout for making gradient measurements	68
30. Effect of various multipoles on the gradient vs position in the magnet aperture	71
31. (a) Achromatic quadrupole lens with poles and electrodes of hyperbolical form	75
(b) Achromatic quadrupole lens with enlarged aperture	75

I. INTRODUCTION

In this report the magnetic field measurements in multipole magnetic fields, which are used to measure magnetic field parameters in the strong-focusing lenses for the Stanford two-mile linear accelerator, will be reviewed. Specifically, the theory and the measurement processes used to determine such important parameters as the magnetic center in multipoles, the length of the gradient fields, and the harmonic content in strong-focusing lenses will be described. Finally, the results of these accurate measurements will be related to the optical parameters of the multipole lenses.

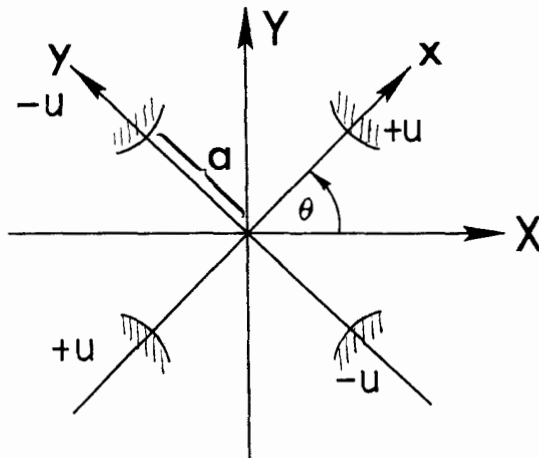
Before starting to describe the individual measurements, a short summary about the properties and field distribution of these lenses will be given.

II. FIELD DISTRIBUTION IN MULTIPOLES

A. The Ideal Quadrupole Magnet

The quadrupole magnet was introduced in 1952 by Courant, Livingston and Snyder¹ along with the strong-focusing synchrotron, and by Christofilos² as a means of focusing charged particle beams. This section will be concerned with the theoretical properties of these lenses and the distribution of their field.

In order to study the field configuration, let us consider the interior of the quadrupole magnet as shown below, which is bounded by four equipotential electrodes maintained respectively at the potential $\pm u$.



Because the interior of the quadrupole is current-free, one can define the scalar magnetic potential which can be calculated from the two-dimensional Laplace equation assuming that the length effect is negligible (infinite length)

$$\nabla^2 u(r, \theta) = r \frac{\partial}{\partial r} \left(r \frac{\partial u}{\partial r} \right) + \frac{\partial^2 u}{\partial \theta^2} = 0$$

Assuming the existence of a product solution in the form

$$u(r, \theta) = R(r)\Theta(\theta)$$

the field equation can be written in the following form:

$$\frac{r}{R} \frac{\partial}{\partial r} \left(r \frac{\partial R}{\partial r} \right) = - \frac{1}{\Theta} \frac{\partial^2 \Theta}{\partial \theta^2}$$

Because the left side of this equation depends only on r and the right side only on θ , both sides must be equal to a constant, k_n^2 . Then

$$\frac{d^2 \Theta}{d\theta^2} + k_n^2 \Theta = 0$$

and

$$r \frac{d}{dr} \left(r \frac{dR}{dr} \right) - k_n^2 R = 0$$

and the solutions of these equations can be written for $k_n \neq 0$

$$\Theta_n = A'_n \cos k_n \theta + B'_n \sin k_n \theta$$

$$R_n = C'_n r^{k_n} + D'_n r^{-k_n}$$

and for $k_n = 0$

$$\Theta_0 = E + F\theta$$

$$R_0 = G + H \ln r$$

Hence the general solution can be written as

$$u = \sum_{n=1}^{\infty} (A'_n \cos k_n \theta + B'_n \sin k_n \theta) \left(C'_n r^{k_n} + D'_n r^{-k_n} \right) + (E + F\theta)(G + H \ln r)$$

Using the following boundary conditions,

$$a. \quad u(r, \theta) = u(r, \theta + 2\pi)$$

$$b. \quad u(r\theta) \text{ must be finite at the origin}$$

$$c. \quad -u(r - \theta) = u(r, \theta) = -u\left(r, \theta + \frac{\pi}{2}\right)$$

one gets from a,

$$F = 0 \quad \text{and} \quad k_n - s \quad \text{are integers}$$

from b,

$$H = D' = 0$$

from c,

$$EG = A = 0 \quad \text{and} \quad n = 2, 6, 10, 14 \dots$$

Then the magnetic potential is given by

$$u_2(r, \theta) = \sum_{n=2,6,10}^{\infty} B_{2n} (\sin n\theta) r^n$$

and the magnetic field intensity is

$$\vec{H} = -\vec{\nabla}u$$

A constant-gradient quadrupole is one in which the first term is the only non-vanishing term, i.e., $B_{2n} \neq 0$, but $B_{2n} = 0$ for $n = 6, 10, 14, \dots$

It is convenient to express the scalar potential for a quadrupole in the XYZ and xyz coordinate systems. Using the following linear transformation

$$X = r \sin \theta$$

$$Y = r \cos \theta$$

one can express the magnetic potential in the XYZ system as

$$\begin{aligned} u &= B_2 r^2 \sin 2\theta + B_6 r^6 \sin 6\theta + \dots \\ &= 2B_2 r^2 \sin \theta \cos \theta + B_6 r^6 \left\{ 32 \cos^5 \theta \sin \theta - 32 \cos^3 \theta \sin \theta \right. \\ &\quad \left. + 6 \cos \theta \sin \theta \right\} + \dots \\ &= 2B_2 XY + B_6 \left\{ 32Y^5 X - 32Y^3 X(X^2 + Y^2) + 6XY(X^2 + Y^2)^2 \right\} \\ &= 2B_2 XY + 6B_6 XY \left\{ X^4 - \frac{10}{3} X^2 Y^2 + Y^4 \right\} + \dots \end{aligned}$$

In the xyz coordinate system, using the following linear transformations

$$\begin{pmatrix} X \\ Y \end{pmatrix} = \begin{pmatrix} \cos(-45^\circ) & \sin(-45^\circ) \\ -\sin(-45^\circ) & \cos(-45^\circ) \end{pmatrix} \begin{pmatrix} x \\ y \end{pmatrix} = \begin{pmatrix} \frac{1}{2} \sqrt{2}x - \frac{1}{2} \sqrt{2}y \\ \frac{1}{2} \sqrt{2}x + \frac{1}{2} \sqrt{2}y \end{pmatrix}$$

one obtains

$$u(x,y) = B_2(x^2 - y^2) + 3B_6 \left[x^6 - 15x^2y^2(x^2 - y^2) - y^6 \right] + \dots$$

Similarly, for a "constant" gradient sextupole and octupole where $\frac{B(a)}{a^2} = \text{const}$ and $\frac{B(a)}{a^3} = \text{const}$ (a = semi-aperture of the system), the magnetic potential in the XYZ system can be written as

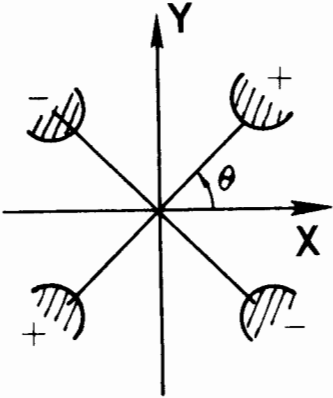
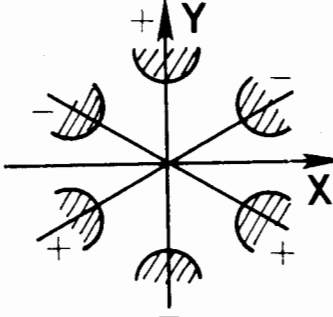
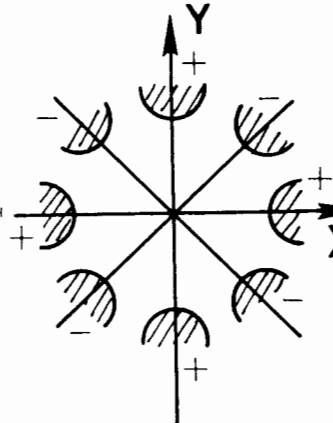
$$\begin{aligned} u_p &= B_3(\sin 3\theta)r^3 = B_3r^2X \frac{\sin 3\theta}{\sin \theta} \\ &= B_3r^2X \frac{3 \sin \theta - 4 \sin^3 \theta}{\sin \theta} \\ &= B_3r^2X \left\{ 1 + 2(\cos^2 \theta - \sin^2 \theta) \right\} \\ &= B_3r^2X \left\{ 1 + 2 \left(\frac{Y^2}{r^2} - \frac{X^2}{r^2} \right) \right\} \\ &= B_3(3Y^2X - X^3) = B'_3(Y^2X - \frac{1}{3} X^3) \end{aligned}$$

for the sextupole and

$$\begin{aligned} u_p &= B_4(\cos 4\theta)r^4(8 \cos^4 \theta - 8 \cos^2 \theta + 1) \\ &= B_4Y^4 \left(8 - \frac{8}{\cos^2 \theta} + \frac{1}{\cos^4 \theta} \right) \\ &= B_4Y^4 \left(8 - \frac{8(X^2 + Y^2)}{Y^2} + \frac{X^4 + Y^4 + 2X^2Y^2}{Y^4} \right) \\ &= B_4(X^4 + Y^4 - 6X^2Y^2) \end{aligned}$$

for the octupole.

The magnetic potential for higher poles can be calculated in a similar manner, using the symmetry conditions to reduce the general solution. In the following table we list the symmetry properties and magnetic scalar potentials for quadrupole, sextupole, and octupole.

Multipole	Symmetry properties of u	Magnetic scalar potential $u(r, \theta)$
<div style="display: flex; align-items: center;"> <div style="writing-mode: vertical-rl; transform: rotate(180deg); margin-right: 10px;">Quadrupole</div>  </div>	$u_2(r, \theta) = -u_2\left(r, \theta + \frac{\pi}{2}\right)$ $= -u_2(r, -\theta)$	$u_2 = \sum_{n=2,6,10}^{\infty} B_2 n (\sin n\theta) r^n .$ <p>For constant gradient</p> $u_{2p} = B_2 (\sin 2\theta) r^2 .$ <p>In the XYZ system</p> $u_{2p} = 2B_2 XY$ $+ 6B_6 XY \left\{ X^4 - \frac{10}{3} X^2 Y^2 + Y^4 \right\}$ $+ \dots$
<div style="display: flex; align-items: center;"> <div style="writing-mode: vertical-rl; transform: rotate(180deg); margin-right: 10px;">Sextupole</div>  </div>	$u_3(r, \theta) = -u_3\left(r, \theta + \frac{\pi}{3}\right)$ $= -u_3(r, -\theta)$	$u_3 = \sum_{n=3,9,15}^{\infty} B_3 n (\sin n\theta) r^n$ $u_{3p} = B_3 (\sin 3\theta) r^3$ $= B_3 (3Y^2 X - X^3)$ $= B'_3 (Y^2 X - \frac{1}{3} X^3)$
<div style="display: flex; align-items: center;"> <div style="writing-mode: vertical-rl; transform: rotate(180deg); margin-right: 10px;">Octupole</div>  </div>	$u_4(r, \theta) = -u_4\left(r, \theta + \frac{\pi}{4}\right)$ $= -u_4(r, -\theta)$	$u_4 = \sum_{n=4,12,20}^{\infty} B_4 n (\cos n\theta) r^n$ $u_{4p} = B_4 (\cos 4\theta) r^4$ $= B_4 (X^4 + Y^4 - 6X^2 Y^2)$

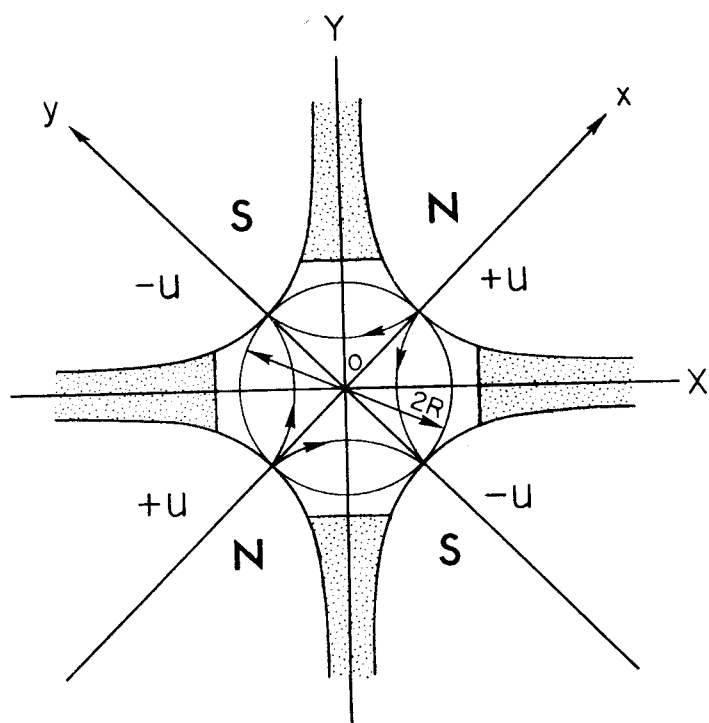
B. Origins of Higher Poles in Quadrupole Magnets

Thus far our discussion has been concerned only with pure multipoles, whereas in practice there is some higher pole content in every multipole magnet. We will briefly discuss qualitatively the source of these higher poles.

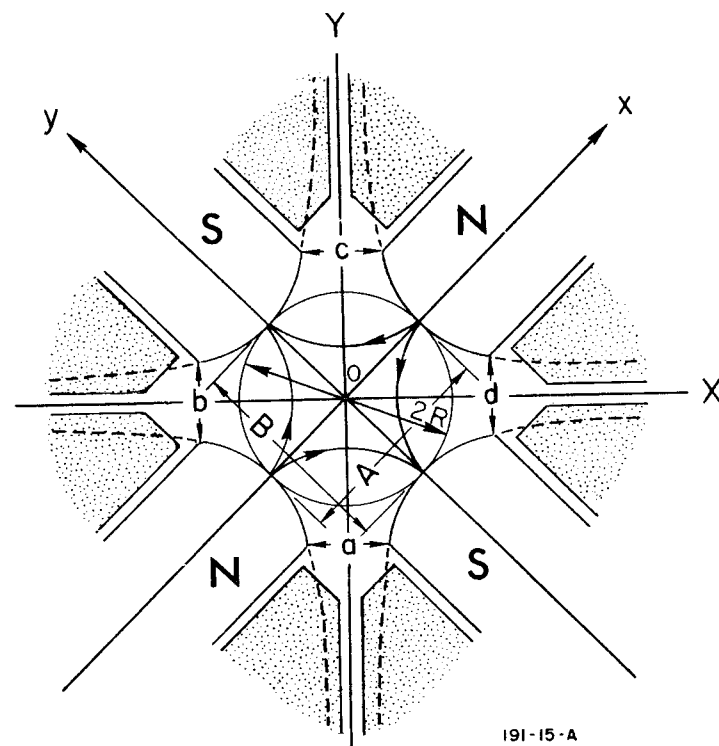
In order to see more clearly how these higher poles occur and how they affect the field distribution of a given magnet, let us discuss here a "practical" quadrupole and the origins of the higher poles in it. (The term "practical" quadrupole refers to one that can be built and used as an optical element in a beam transport system.) Figure 1 shows some of the differences between an ideal quadrupole and a practical one. One can see that in the practical quadrupole the pole surfaces have the required hyperbolic shape over a considerable extent, but must be truncated laterally at some point to allow sufficient space for the excitation windings. In the ideal quadrupole the pole surfaces are shaped according to the equation $X \cdot Y = \pm R^2/2$. In order to discuss the effects of mechanical imperfections in the practical magnet, we will designate the pole tip spacing along X as A and the pole tip spacing along Y as B. Let the letters a, b, c, and d stand for the spacing between adjacent poles measured at the point of truncation (see Fig. 2).

C. Origins of Poles with Four-fold Symmetry

We shall first concern ourselves with a mechanically perfectly fabricated quadrupole as far as symmetry of the location of the four poles is concerned, that is, where $A = B = 2R$ and $a = b = c = d$. In this case, the fabrication of the poles themselves would be the only source of the higher poles. Let us further assume that the poles themselves are perfectly symmetrical about their own centerline axes along X and Y. The fact that the extent of the hyperbolic pole pieces is not infinite would result in a pole configuration that has the four-fold quadrupole symmetry; however, because the magnetic equipotential of the pole stops at the point of truncation, the field would appear too low at the truncation. These truncations then result in a situation like that in Fig. 2 (which depicts one pole only). Near the points of truncation, the field of the pole (N) suffers a weakening of the N field and can

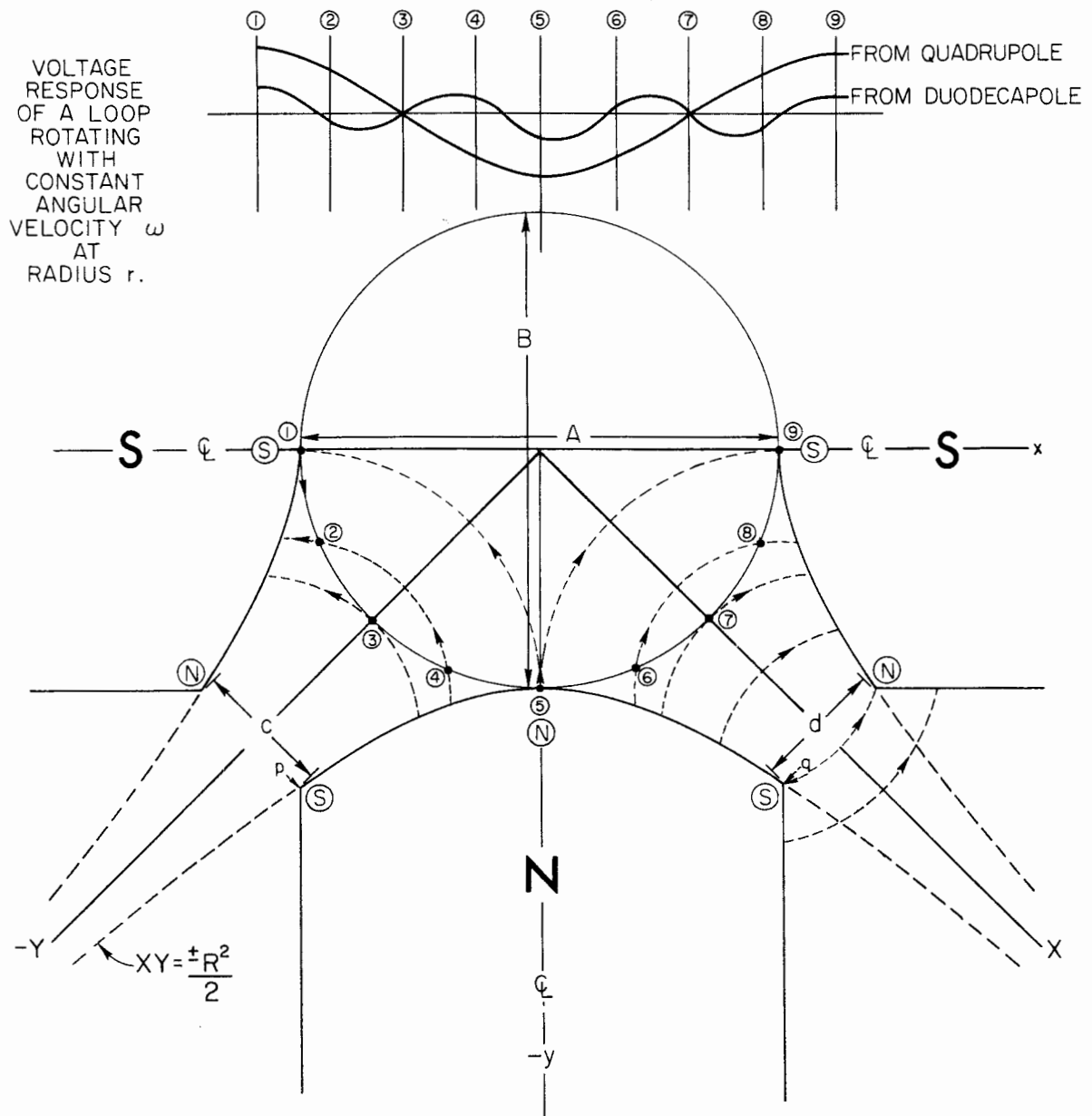


a) IDEAL (THEORETICAL) QUADRUPOLE



b) PRACTICAL QUADRUPOLE. THE SHAPE OF THE POLE SURFACES DOES NOT EXACTLY CORRESPOND TO A TRUE HYPERBOLA AND THE POLES HAVE BEEN TRUNCATED Laterally TO PROVIDE SPACE FOR COILS.

FIG. 1



191-16-A

FIG. 2 - QUADRUPOLE CONSTRUCTED PERFECTLY WITH HYPERBOLIC POLES
BUT POLES TRUNCATED AT POINTS p AND q.

be represented as a virtual S field superimposed on the N field. The cause of this weakening can be attributed to two factors, a leakage of flux beyond the truncation point and a saturation of the pole at the truncation point. The multipole so produced is the duodecapole, as each pole acts as three poles. The factor causing the duodecapole field can be ascertained by examining the percent of duodecapole field at various magnet excitation currents. If the cause is field leakage, the percent of duodecapole will be found to be constant with different magnet strengths. If saturation at points p and q is the cause of the duodecapole field the percent of duodecapole will be current dependent; thus, the duodecapole percent will increase with magnet strength.

If the pole is made by taking a circular approximation to the required hyperbolic shape, even higher poles will be present in the quadrupole. If the pole is made symmetrically, these higher poles will result in some of each of the possible poles having four-fold symmetry, that is, each will have an odd number of poles in each quadrant. Therefore, the higher poles that can possibly exist in the magnet when all elements of construction are perfect (i.e., $A = B = 2R$ and $a = b = c = d$) are 4-pole, 12-pole, 20-pole, 28-pole, or $4(2n - 1)$ poles where $n = 1, 2, 3 \dots$. Figure 3 illustrates that, by using a circular shape on the pole as an approximation to the ideal hyperbola, the resultant pole is rich in 12-pole and 20-pole.

From this discussion one can see how the shape of the pole itself can contribute to many combinations of higher poles with four-fold symmetry.

D. Origins of Poles with Two-fold Symmetry

Thus far the origins of only those poles with four-fold symmetry have been explained and we have concerned ourselves only with those cases where the quadrupole is symmetrically assembled mechanically. Now let us assume that the poles are perfect hyperbolas but that the mechanical construction is such that the opposite pole spacing A is not equal to B, but $a = b = c = d$. An exaggerated picture of this situation is shown in Fig. 4. This is only one way in which the octupole perturbation can be generated. The other usual way is when $A = B$, $a = c$,

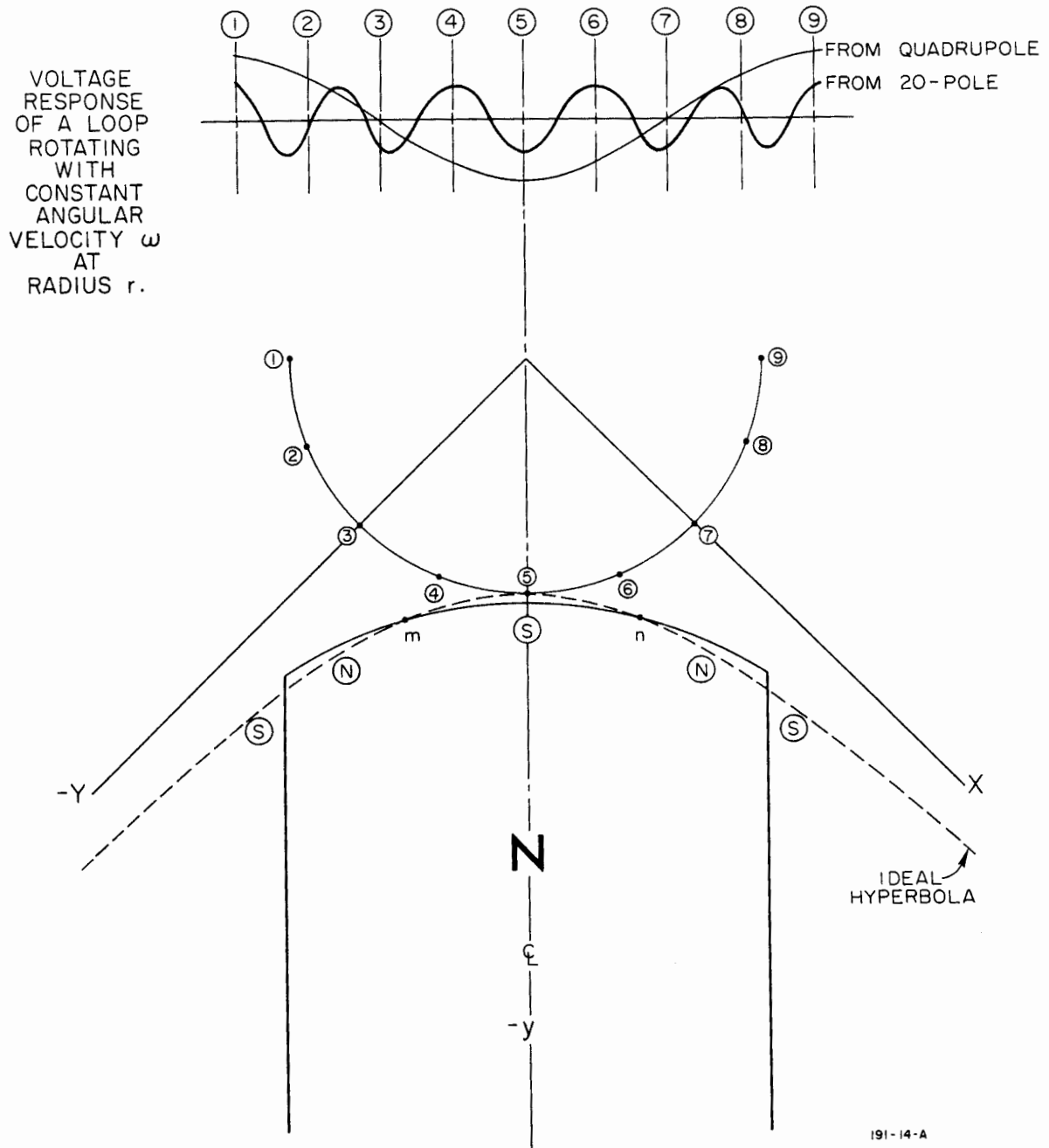


FIG. 3 - QUADRUPOLE CONSTRUCTED WITH CIRCULAR APPROXIMATION TO IDEAL HYPERBOLIC SHAPE. CIRCLE AND HYPERBOLA COINCIDE AT POINTS m AND n .

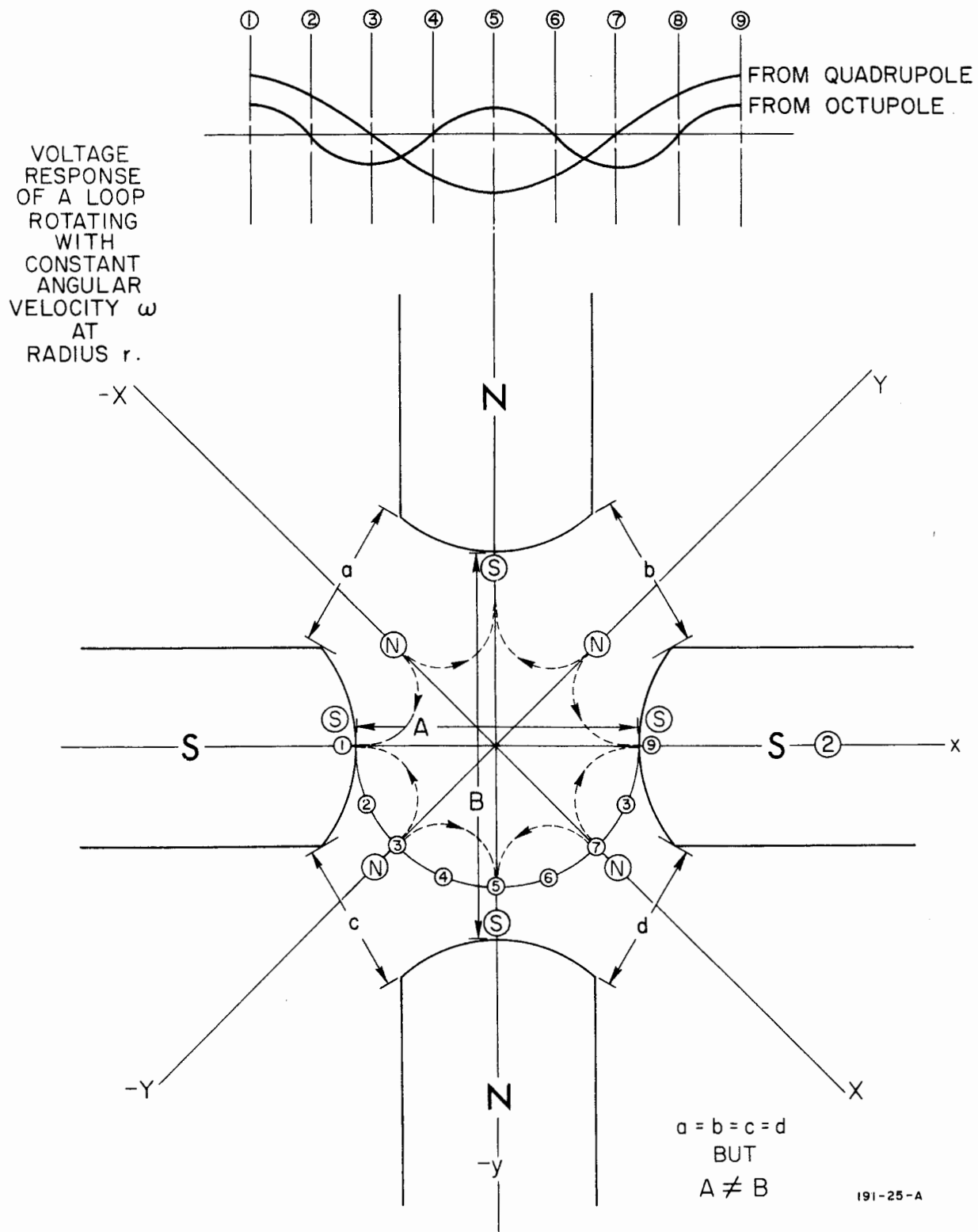


FIG. 4 - OCTUPOLE PERTURBATION IN A QUADRUPOLE FIELD GENERATED BY GEOMETRICAL ASYMMETRY ($a = b = c = d$, BUT $A \neq B$)

and $b = d$, but $a \neq b$. Such a situation is shown in Fig. 5. Here again octupole is present, but the octupole contribution is of different phase from the previous example. From a slight extension of this analysis one can see how these misalignments can account for the whole set of multipoles with two-fold symmetry. These are the multipoles contained in the set octupole, 16-pole, 24-pole, 32-pole, or $2(4n)$ poles where $n = 1, 2, 3, \dots$.

E. Origins of Asymmetric Poles

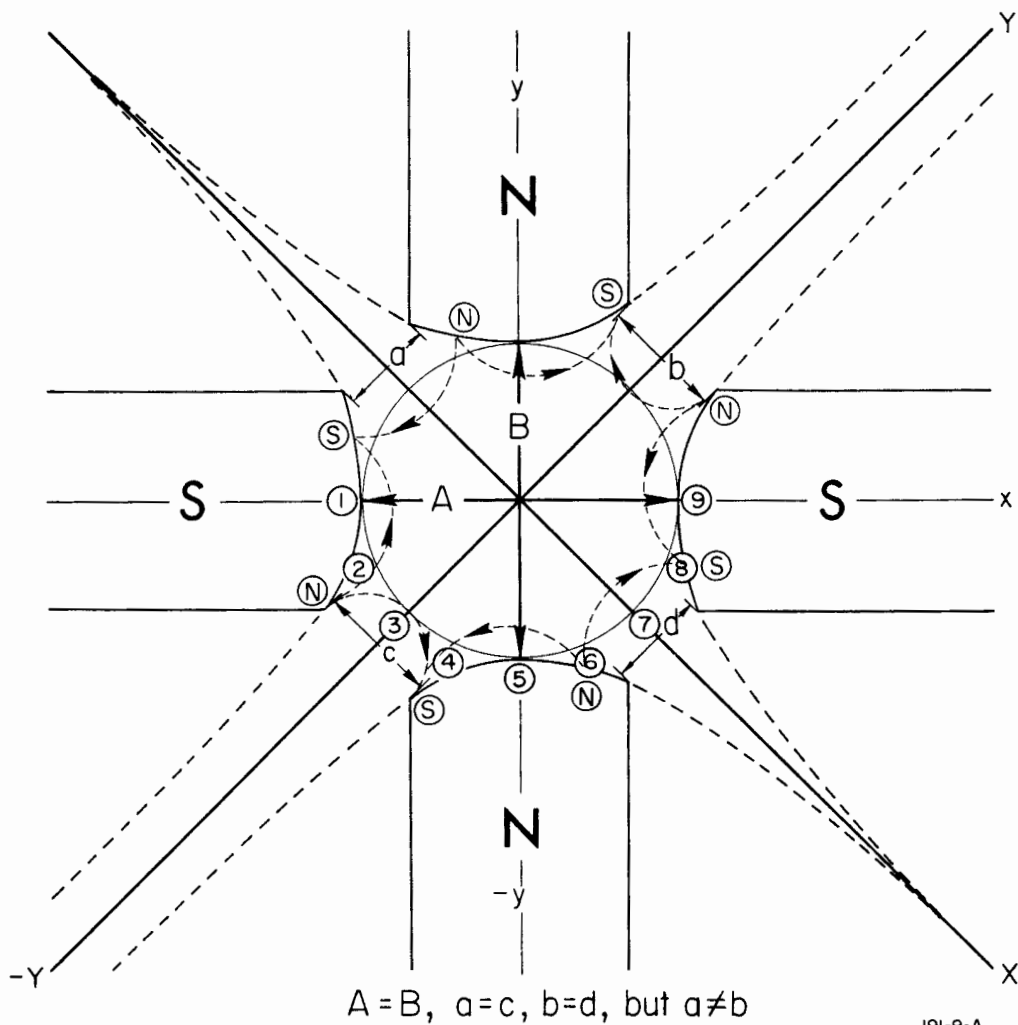
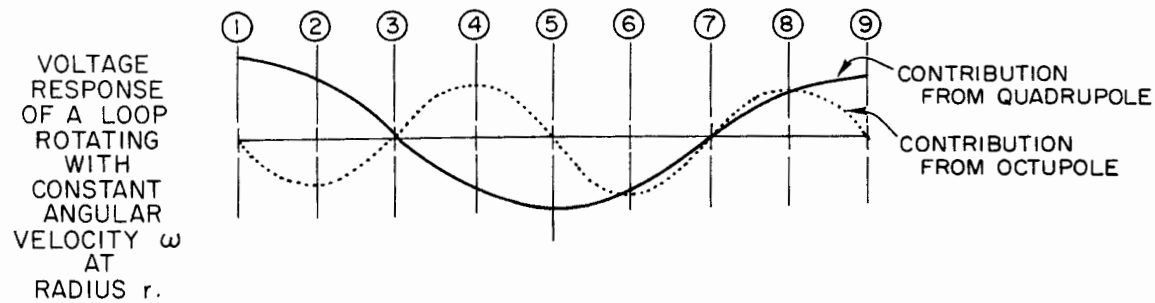
In quadrupoles so constructed that $a \neq c$ or $b \neq d$, various higher poles can occur; these are in general poles that are asymmetric, that is they have neither two- nor four-fold symmetry. These poles are the dipole, sextupole, decapole, 14-pole, 18-pole, or $2(4n \pm 1)$ poles where $n = 0, 1, 2, 3, \dots$, and there are an equal number of these asymmetric higher poles as there are poles with two- or four-fold symmetry. Figure 6 shows an asymmetric perturbation in a quadrupole and illustrates the source of the dipole and sextupole in a quadrupole magnet.

III. MAGNETIC CENTER LOCATION

A. Experimental

The magnetic center of a quadrupole magnet does not necessarily correspond to the mechanical center. For alignment of a quadrupole one must know the relationship of the magnetic center to the mechanical center. Of the many methods of determining the magnetic center of a quadrupole, three will be discussed here.

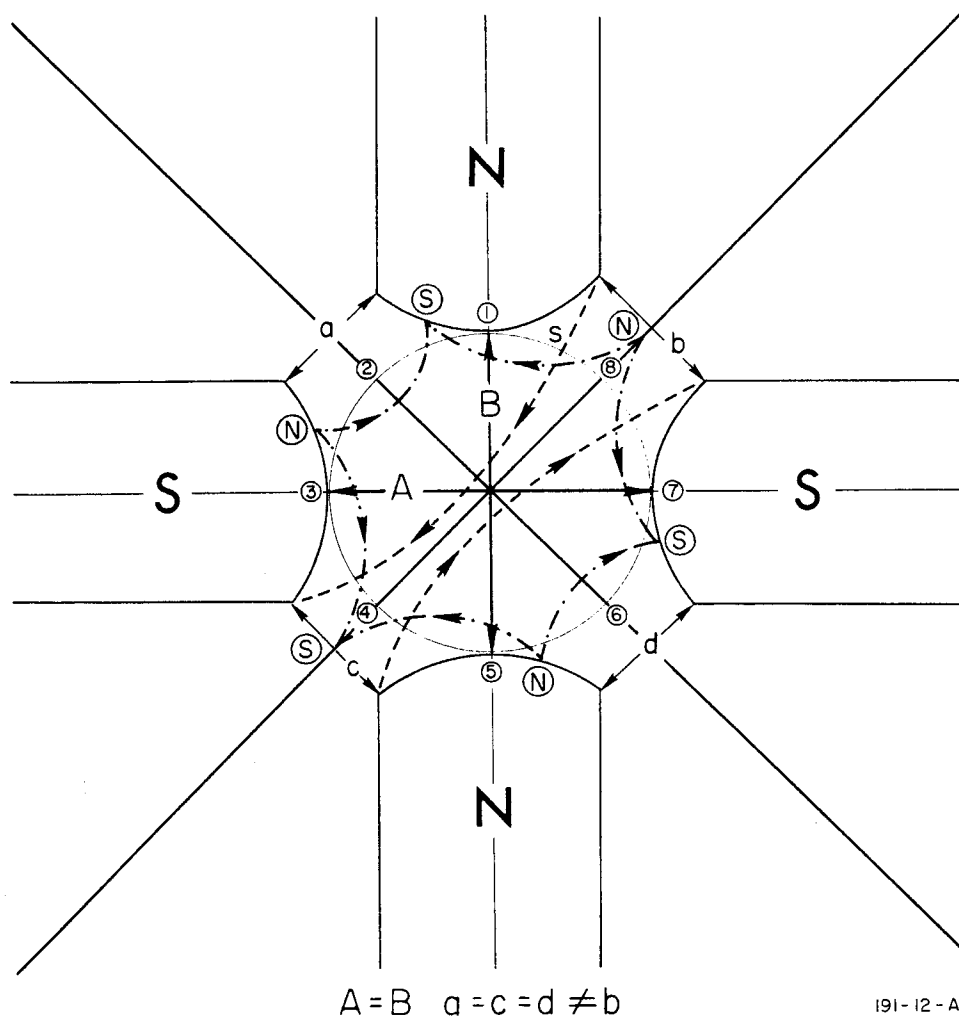
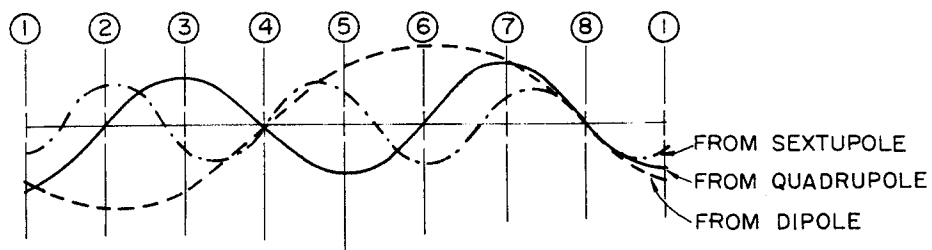
Rotating coils provide one method of determining the magnetic center of a quadrupole. Since the field at the center of a quadrupole is zero, the output from a rotating coil is zero when the axis of the coil coincides with the magnetic center of the quadrupole. With a symmetrical rotating coil the method is reasonably simple since the quadrupole field induced voltage is canceled by the symmetry of the coil and the output is proportional to the magnitude of the dipole field which is strictly a function of position. The accuracy of this method of locating the magnetic center is no better than several thousandths of an inch because of uncertainties in the coil geometry, coil vibrations, and runout of the coil shaft.



191-9-A

FIG.5 OCTUPOLE PERTURBATION IN A QUADRUPOLE FIELD GENERATED
BY GEOMETRICAL ASYMMETRY ($A=B, a=c, b=d, \text{ but } a \neq b$).

VOLTAGE
RESPONSE
OF A LOOP
ROTATING
WITH
CONSTANT
ANGULAR
VELOCITY ω
AT
RADIUS r .



191-12-A

FIG. 6 DIPOLE AND SEXTUPOLE FIELDS GENERATED BY ASYMMETRIC PERTURBATION IN A QUADRUPOLE.

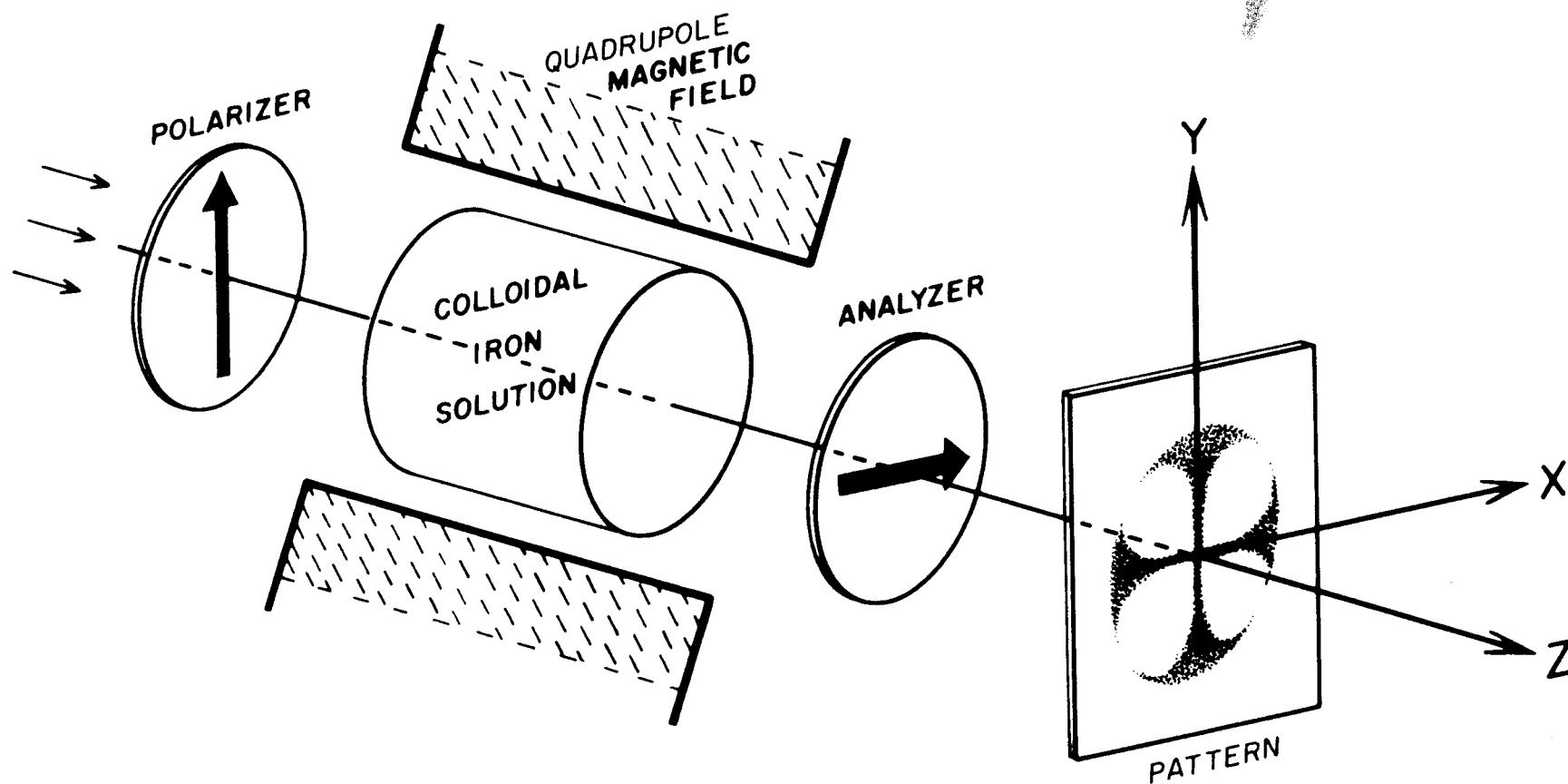
A floating wire is another method of center determination for a quadrupole. This involves putting a taut wire through the magnet at the approximate center. First, the magnet is energized, then a current is passed through the taut wire, and deflection of the wire is noted as evidence that the wire is not at the magnetic center. The wire is then moved and the process repeated until no deflection of the wire is observed as the wire current is turned on. The wire is then in the magnetic center. The floating wire technique is probably good for center location to an accuracy of a few mils, but requires a considerable amount of elaborate equipment.

The third, and in our case the most important method of magnetic center determination, is the use of a colloidal suspension of ferrous oxide particles. This technique was proposed and used by R. M. Johnson³ to locate the magnetic center of quadrupole fields. The physical mechanism of this method was explained recently⁴ as scattering of polarized light on aligned colloidal particles in multipole fields. In this system a small vial of the suspension is placed in the magnetic quadrupole field such that the mechanical center falls within the area of the vial. White plane-polarized light is directed through the vial of solution from one end of the magnet. The experimental arrangement is shown in Fig. 7.

The observer at the opposite end of the magnet then looks at the vial through a plane-polarizing analyzer which is aligned with the polarizer of incoming light such that complete cancellation of light should occur when the magnetic field is turned off. With magnetic field, complete cancellation does not occur except along two mutually perpendicular axes which cross at the magnetic center of the quadrupole. The accuracy of this type of center determination is of the order of ± 0.001 inch.

Typical scattering patterns in multipole fields are shown in Fig. 8 for a quadrupole field, in Fig. 9 for a sextupole field, and in Fig. 10 for octupole fields.

The scattering centers in the colloidal solution are Fe_3O_4 crystallites. The preparation of such a colloidal solution is described by D. J. Craik and P. M. Griffiths.⁵ The individual crystallites of the magnetite (Fe_3O_4) have been measured with an electron microscope by Craik⁶ and it was found that the particles are of the order of 100\AA .



136-I-A

FIG.7 -EXPERIMENTAL SETUP FOR MAGNETIC CENTER LOCATION IN QUADRUPOLE MAGNETIC FIELD.

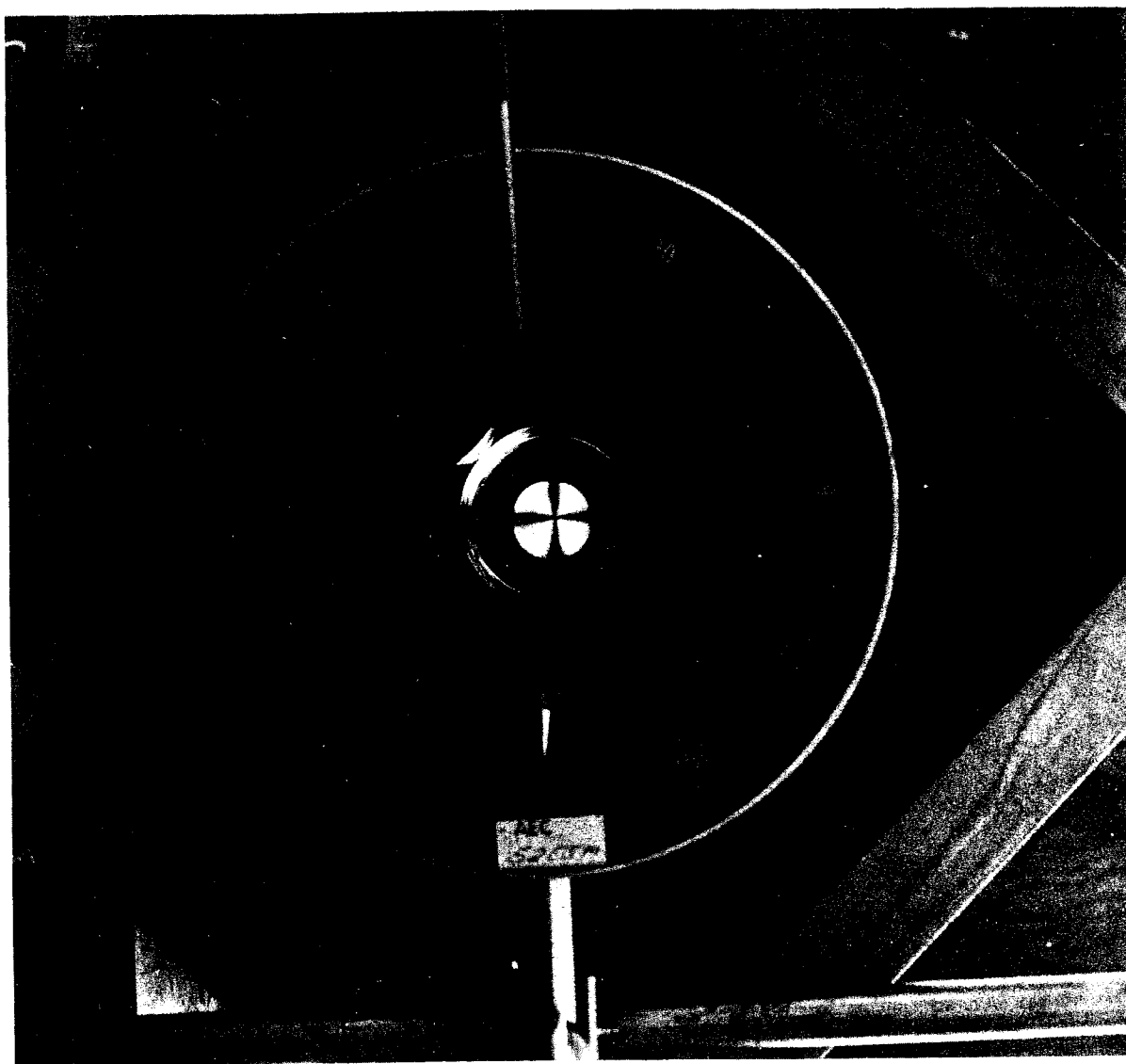


FIG. 8--Light scattering pattern in a quadrupole magnetic field.
($\theta = 90^\circ$)

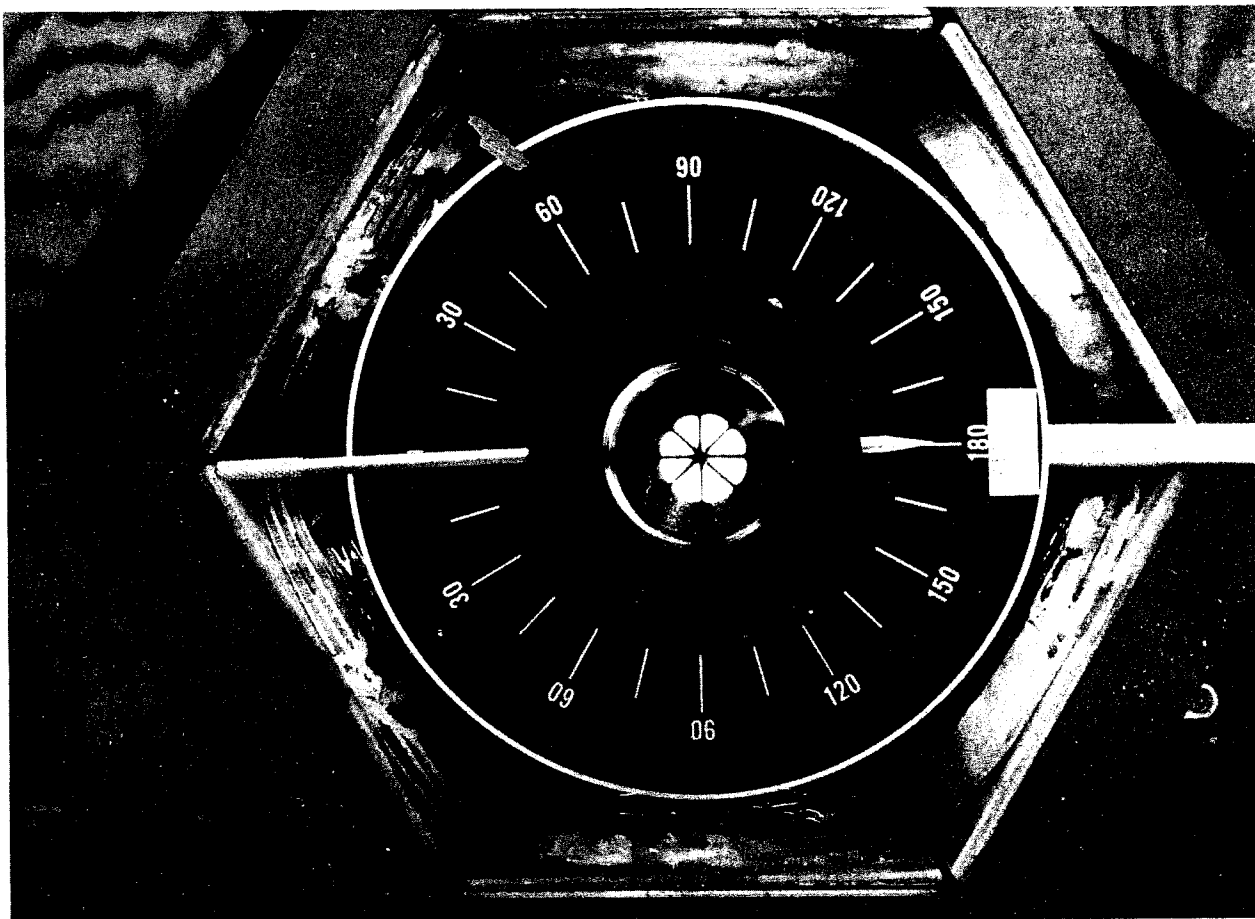


FIG. 9--Light scattering pattern in a sextupole magnet field.
($\theta = 0$)

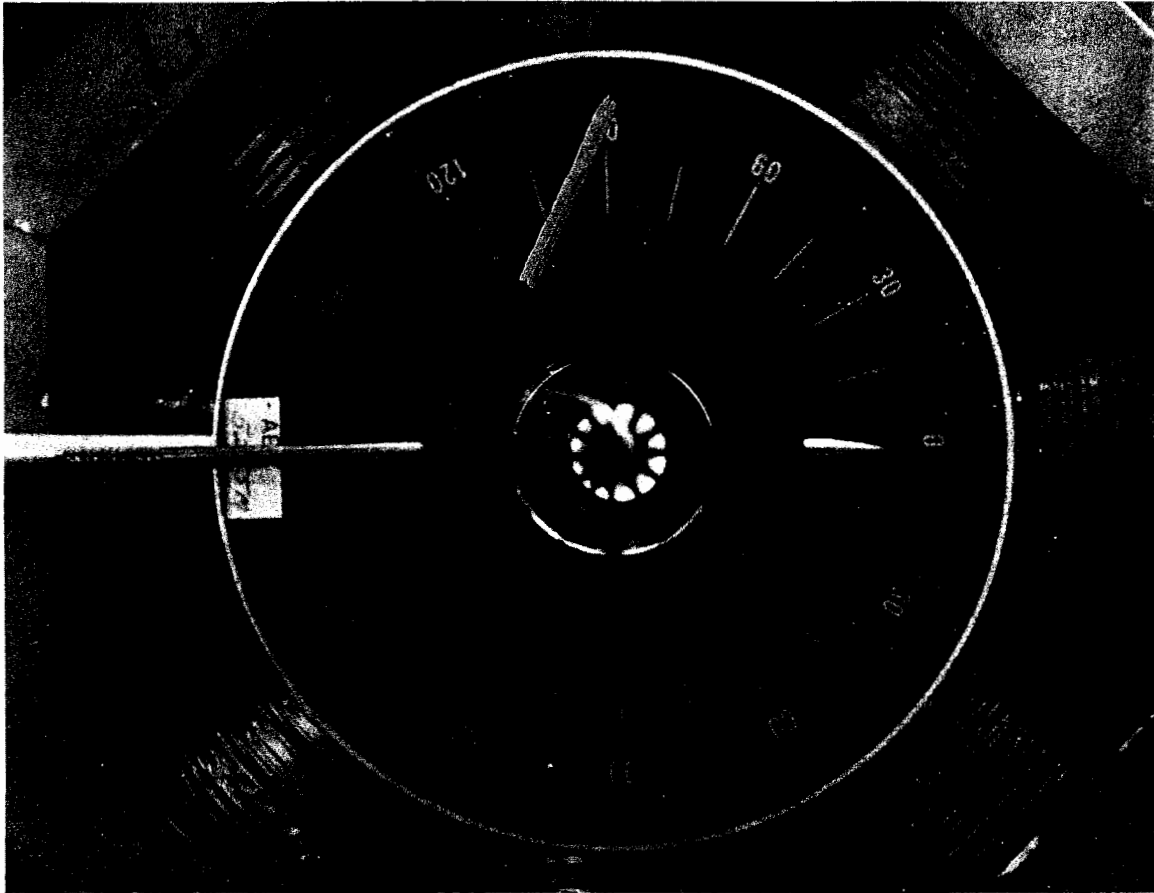


FIG. 10--Light scattering pattern in an octupole magnetic field.
($\theta = 0$)

The alignment of these magnetite crystallites in the magnetic field might be explained by the theory of paramagnetic alignment. If N_0 is the number of crystallites per unit volume, the number of aligned scattering centers is given by the following formula

$$N = N_0 L(a) = N_0 \left[\cosh \frac{mH}{kT} - \frac{kT}{mH} \right] ; \quad a = \frac{mH}{kT}$$

where m is the magnetic moment of the colloidal particle, H is the applied field, T is the temperature of the solution, and $L(a)$ is the well-known Langevin function used in the classical theory of paramagnetism. In the case of very strong field or very low temperature, the Langevin function becomes unity, so

$$N = N_0 = N_{\text{sat}}$$

If all the dipoles are aligned with the field, the number of scattering centers is independent of the applied field, that is, the number of scattering centers is saturated.

The dependence of the sharpness of the scattering pattern on temperature and field can be easily observed by a simple experimental setup, such as that shown in Fig. 7.

B. Symmetry Relations in Multipole Fields

The theory of anisotropic light scattering is very complicated and a rigorous solution of the problem exists only in a few special cases. In this case the symmetry properties of the magnetic multipoles allow a number of simplifications in the calculation of the intensity distribution of the scattering pattern. Such a symmetry relation in a quadrupole field is that any line passing through the center of symmetry with an angle θ , with respect to the X axis, will cross the magnetic field lines at an angle β , where

$$\beta = -\frac{\pi}{2} + 2\theta$$

In order to prove this relation, write the magnetic field in a quadrupole in the following form

$$\vec{H} = - \vec{i} \frac{\partial u}{\partial X} - \vec{j} \frac{\partial u}{\partial Y}$$

where $u = 2B_2XY$ is the scalar magnetic potential. Thus

$$\vec{H} = 2(\vec{i}Y + \vec{j}X)$$

The line which gives the direction of the magnetic field at point Q intersects the X axis with an angle γ (see Fig. 11) which is given by

$$\tan \gamma = \frac{(\vec{H})_Y}{(\vec{H})_X} = \frac{X}{Y} = \frac{r \cos \theta}{r \sin \theta} = \cot \theta = \tan(\pi/2 - \theta)$$

or

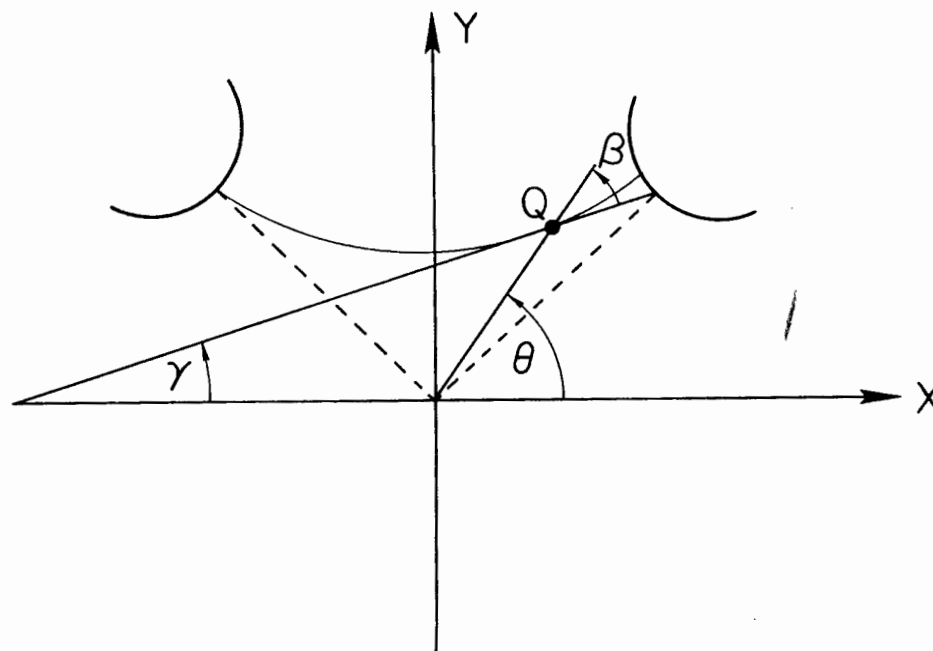
$$\gamma = \pi/2 - \theta$$

Hence, since $\gamma + \pi - \theta + \beta = \pi$,

$$\beta = \frac{\pi}{2} + 2\theta$$

But β is defined as the angle between two vectors; therefore, one must consider β and $\beta + \pi$ as the angles between the direction of the magnetic field line at point Q and the line passing through the center. This yields

$\beta = \frac{\pi}{2} + 2\theta$ $\beta = -\frac{\pi}{2} + 2\theta$
--



191-7-A

FIG.II - INTERRELATION OF ANGLES γ , θ , AND β IN
A MAGNETIC FIELD WITH QUADRUPOLE SYMMETRY.

A similar analysis can be carried out in the case of the sextupole field. There

$$\vec{H} = -B'_3 \left\{ \vec{i}(-2XY) + \vec{j}(Y^2 - X^2) \right\}$$

This leads to

$$\begin{aligned} \tan \gamma &= \frac{H_Y}{H_X} = \frac{Y^2 - X^2}{-2XY} = \frac{r^2 \sin^2 \theta - r^2 \cos^2 \theta}{-2r^2 \cos \theta \sin \theta} \\ &= \frac{-\cos 2\theta}{-\sin 2\theta} = \cot 2\theta = \tan \left(\frac{\pi}{2} - 2\theta \right) \end{aligned}$$

From this one obtains $\gamma = \frac{\pi}{2} - 2\theta$, and $\gamma + \pi - \theta + \beta = \pi$ gives

$$\beta = -\frac{\pi}{2} + 3\theta$$

$$\beta = \frac{\pi}{2} + 3\theta$$

Quite similarly, for an octupole field the magnetic scalar potential can be written as

$$u = B_4(X^4 + Y^4 - 6X^2Y^2)$$

and

$$\vec{B} = -B_4 \left\{ \vec{i}(4X^3 - 12XY^2) + \vec{j}(4Y^3 - 12X^2Y) \right\}$$

and from this we have

$$\begin{aligned}\tan \gamma &= \frac{H_Y}{H_X} = \frac{4Y - 12X^2Y}{4X - 12XY^2} = \frac{r^3 \sin^3 \theta - 3r^3 \cos^2 \theta \sin \theta}{r^3 \cos^3 \theta - 3r^3 \cos \theta \sin^2 \theta} \\ &= - \frac{\sin 3\theta}{\cos 3\theta} = - \tan 3\theta\end{aligned}$$

Then

$$\gamma = - 3\theta$$

and from $\gamma + \pi + \theta + \beta = \pi$, one gets

$\begin{aligned}\beta &= 4\theta \\ \beta &= \pi + 4\theta\end{aligned}$
--

It was observed that the scattering pattern does not change with a change in polarity, which means that a particle aligned parallel with the magnetic field scatters the same way in the scattering process as a particle that is aligned opposite to the field. Particles with induced magnetic moments are aligned along the field lines irrespective of the relative directions of the magnetic field \vec{H} and the moment \vec{m} . Therefore, the relative orientations of \vec{m} and \vec{H} are not taken into account in further calculations. The symmetry relations used for the following calculations can be written as

$\beta = 2\theta$	for quadrupole fields
$\beta = 3\theta$	for sextupole fields
$\beta = 4\theta$	for octupole fields

C. Theory of Light Scattering on Aligned Particles in Multipole Fields

In order to explain the intensity distribution of the scattered polarized light on the aligned magnetite crystallites, one can assume anisotropy in the scattering process. One of the simplest assumptions is that the aligned magnetite has a different polarizability along the magnetic field than it does perpendicular to the field. The net effect of this anisotropy in the scattering is a rotation of the initial angle of polarization along certain lines going through the center of the multipole fields. The polarizability tensor in the coordinate system of the aligned particle ($X'-Y'$) can then be written as

$$\alpha_{ik} = \begin{vmatrix} \alpha_{\perp} & 0 \\ 0 & \alpha_{\parallel} \end{vmatrix}$$

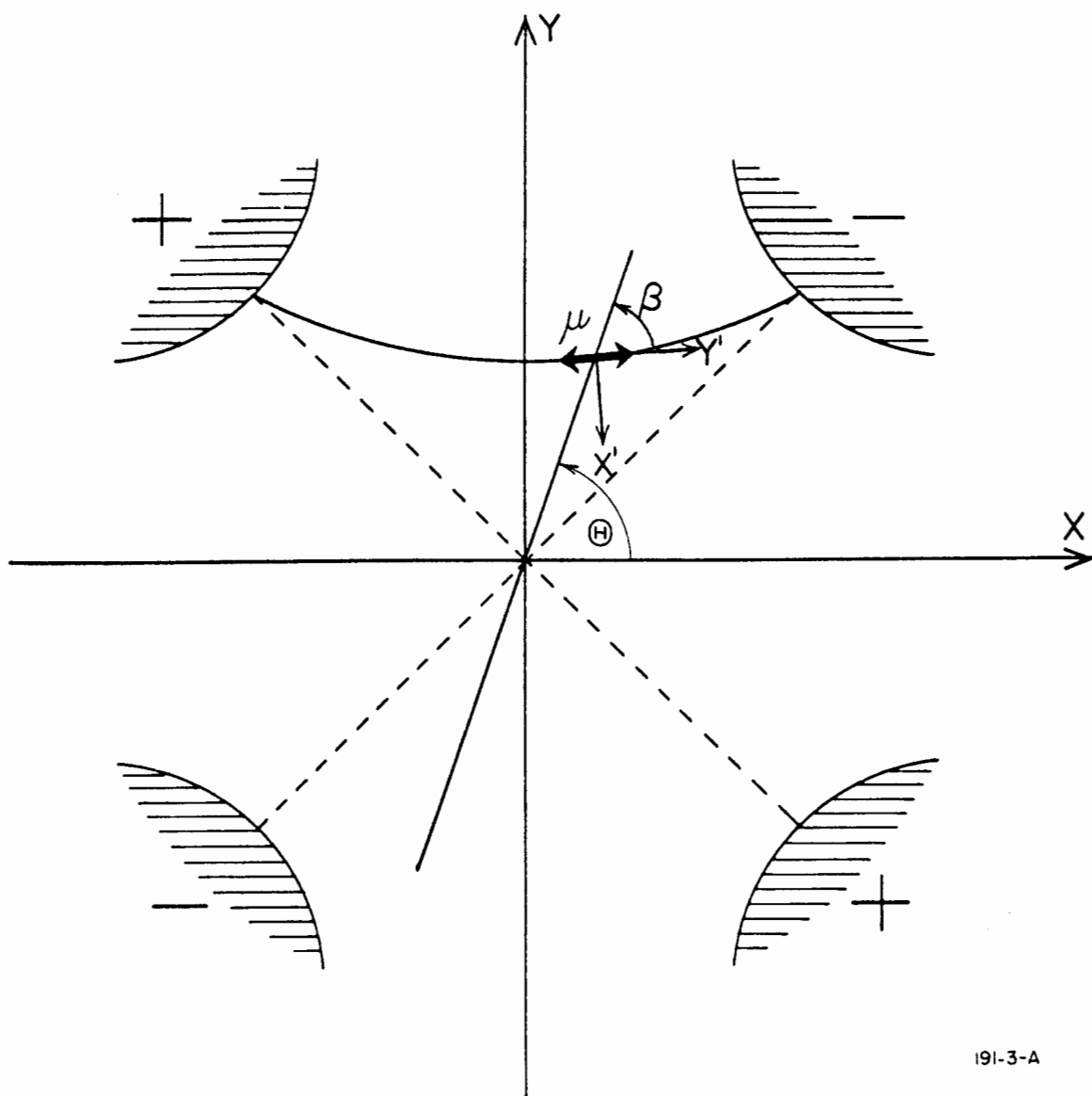
In order to calculate the polarizability tensor in the $X-Y$ coordinate system, it is desirable to use the symmetry properties of the multipole fields. Figure 12 shows the relative orientation of the ($X'-Y'$) coordinate system, where

$$\alpha_{ik} = \begin{vmatrix} \alpha_{\perp} & 0 \\ 0 & \alpha_{\parallel} \end{vmatrix}$$

to the ($X-Y$) system in a quadrupole magnetic field.

With these relationships, the polarizability tensor in the $X-Y$ system can be expressed using a rotational transformation (see Fig. 12):

$$|\alpha_{ik}|_{XY} = S \left(\frac{\pi}{2} - \theta + \beta \right) \begin{vmatrix} \alpha_{\perp} & 0 \\ 0 & \alpha_{\parallel} \end{vmatrix}$$



191-3-A

FIG. 12 ORIENTATION FOR A MAGNETIC DIPOLE μ IN A MAGNETIC FIELD WITH QUADRUPOLE SYMMETRY.

where $S(\theta + \beta)$ is the transformation matrix, i.e.,

$$S(\theta + \beta) = \begin{pmatrix} \cos(\frac{\pi}{2} - \theta + \beta) & -\sin(\frac{\pi}{2} - \theta + \beta) \\ \sin(\frac{\pi}{2} - \theta + \beta) & \cos(\frac{\pi}{2} - \theta + \beta) \end{pmatrix}$$

Using $|\alpha_{ik}|_{XY}$, all quantities can be expressed in the X-Y coordinate system and the scattering amplitude can be calculated easily. The size of the scattering centers (100 - 1000 \AA) is small as compared to the polarized light, so the Rayleigh approximation can be used. In this case the total intensity of the scattered light is the sum of the scattered intensities of each of the scattering centers, and the scattering amplitude by the i-th volume element of the system at the location of the observer is given⁷ as

$$A_i = K(\vec{P}_i \cdot \vec{O}) \cos k(\vec{r}_i \cdot \vec{s})$$

The induced dipole in the i-th volume element is \vec{P}_i , which is located a distance r_i from the origin $k = 2\pi/\lambda$ (λ = wavelength in the medium); $\vec{s} = \vec{s}' - \vec{s}_0$ where \vec{s}' and \vec{s}_0 are unit vectors along the scattered and incident beams; \vec{O} is the unit vector perpendicular to the scattered light beam and along the polarization direction of the scattered light; K is a proportionality constant.

The dipole moment P_i is given by

$$P_i = \alpha_{ik} E_K$$

In the X-Y coordinate system the components of \vec{E} are given as

$$\vec{E} = E_0 \left[(\cos \varphi) \vec{i} + (\sin \varphi) \vec{j} \right]$$

where φ is the angle of polarization. The components of \vec{O} can be

expressed as

$$\vec{O} = \left[(\sin \varphi) \vec{i} - (\cos \varphi) \vec{j} \right]$$

when observation is perpendicular to the X-Y plane and along the symmetry axis of the multipoles. In this case

$$\vec{s}' = \vec{s}_0 \quad \text{and} \quad \cos k(\vec{r}_i \cdot \vec{s}) = 1$$

The total amplitude of the scattered light from the X-Y plane can be written

$$A = \Sigma A_i = K' \int_{r=0}^R \int_{\varphi=0}^{2\pi} (\vec{O} \cdot \vec{P}) r dr d\varphi$$

By squaring the total amplitude, the intensity is obtained.

The angle θ relative to the X axis at which the intensity is zero for a given polarization angle φ is given by the expression

$$(\vec{P} \cdot \vec{O}) = P_X \sin \varphi - P_Y \cos \varphi = 0$$

Scattering processes in different multipoles will now be considered.

D. Light Scattering on Aligned Particles in a Quadrupole Field

In a quadrupole field, the dielectric tensor in the X-Y system can be written as

$$\alpha_{ik} \Big|_{XY} = S \left(\frac{\pi}{2} - \theta + \beta \right) \begin{vmatrix} \alpha_{\perp} & 0 \\ 0 & \alpha_{\parallel} \end{vmatrix} = S(\theta) \begin{vmatrix} \alpha_{\perp} & 0 \\ 0 & \alpha_{\parallel} \end{vmatrix}$$

and the induced dipole moment as

$$\vec{P} = |\alpha|_{XY} \vec{E} = \begin{pmatrix} \alpha_{\perp} \cos \theta \cos \varphi - \alpha_{\parallel} \sin \theta \sin \varphi \\ \alpha_{\perp} \sin \theta \cos \varphi + \alpha_{\parallel} \cos \theta \sin \varphi \end{pmatrix}$$

With the above, and using the condition for zero intensity

$$(\vec{P} \cdot \vec{O}) = P_X \sin \varphi - P_Y \cos \varphi = 0$$

one obtains θ in terms of φ :

$$\begin{aligned} \alpha_{\perp} \tan \varphi &= \alpha_{\perp} \tan \theta \\ \alpha_{\parallel} \tan \varphi &= \alpha_{\perp} \tan(90^\circ + \theta) \end{aligned}$$

From the experimental observation, the location of the two dark lines as functions of the polarization angle (φ) are consistent within the experimental error with the following equations

$$\tan \varphi = \tan \theta$$

$$\tan \varphi = \tan(90^\circ + \theta)$$

The scattering intensity is proportional to the square of the amplitude; consequently,

$$I_1 \alpha A_1^2 = K^2 (\vec{O} \cdot \vec{P})^2$$

The numerical value for the constant K might be obtained from the Rayleigh formula, from which

$$K^2 = \frac{8\pi^4}{\lambda^4} N_1 E^2$$

where N_i is the density of scattering centers in volume element V_i , and

$$N_i = N_o \left[\cosh \frac{mH}{kT} - \frac{kT}{mH} \right]$$

Along the Z axis, the scattered light intensity from volume element V_i can be expressed as

$$I = \frac{8\pi^4 N_o E^2}{\lambda^4} \left[\cosh \frac{mH}{kT} - \frac{kT}{mH} \right] \left[\vec{O} \cdot \vec{P} \right]^2$$

E. Light Scattering on Aligned Particles in Sextupole and Octupole Fields

In sextupole and octupole fields, the magnetic field intensity changes as $(B_o/R_o^2)r^2$ and $(B_o/R_o^3)r^3$, respectively, where B_o is the field at the pole faces, R_o is the half-aperture, and $r^2 = X^2 + Y^2$.

Therefore, the magnetic field intensity is very low near the Z axis and is not sufficient to align the scattering centers in the field direction. This might be the reason for the unclear scattering picture near the Z axis as seen in Figs. 9 and 10.

In a sextupole field the dipole moment can be written as

$$\begin{aligned} \vec{P} &= |\alpha|_{XY} \vec{E} = S \frac{\pi}{2} + 2\theta \begin{vmatrix} \alpha_{\perp} & 0 \\ 0 & \alpha_{\parallel} \end{vmatrix} \begin{pmatrix} \cos \varphi \\ \sin \varphi \end{pmatrix} E_o \\ &= E_o \begin{pmatrix} -\alpha_{\perp} \sin 2\theta \cos \varphi & -\alpha_{\perp} \cos 2\theta \sin \varphi \\ \alpha_{\perp} \cos 2\theta \cos \varphi & -\alpha_{\perp} \sin 2\theta \sin \varphi \end{pmatrix} \end{aligned}$$

when the angle of polarization is φ . The azimuth angle θ for zero intensity lines was obtained from

$$(\vec{O} \cdot \vec{P}) = P_X \sin \varphi - P_Y \cos \varphi = 0 ,$$

and with this one finds that

$$\tan \varphi = \tan 2\theta$$

$$\tan \varphi = \tan(90^\circ + 2\theta)$$

Quite similarly, for an octupole field the dipole moment of the aligned colloidal particles can be written as:

$$\vec{P} = |\alpha|_{XY} \vec{E} = \begin{pmatrix} -\alpha_{\perp} \sin 3\theta \cos \varphi & -\alpha_{\parallel} \cos 3\theta \sin \varphi \\ \alpha_{\perp} \cos 3\theta \cos \varphi & -\alpha_{\parallel} \sin 3\theta \sin \varphi \end{pmatrix}$$

from which, using $(\vec{O} \cdot \vec{P}) = 0$, one obtains

$$\tan \varphi = \tan 3\theta$$

$$\tan \varphi = \tan(90^\circ + 3\theta)$$

In both cases the observed locations of dark lines characterized by the azimuth angle θ agree with the calculated values for a given polarization angle φ . At zero polarization angles, as shown in Figs. 9 and 10. the dark lines are located at

$$\theta = 0^\circ, 45^\circ, 90^\circ, \text{ and } 135^\circ$$

for the sextupole field, and at

$$\theta = 0^\circ, 30^\circ, 60^\circ, 90^\circ, 120^\circ, \text{ and } 150^\circ$$

for octupole fields. It is interesting to note that the angular separation of the dark lines is 45° in a sextupole field and 30° in the octupole field (see Figs. 9 and 10).

Table I lists the calculated azimuthal location of the dark lines as a function of the polarization angle $\varphi(0 < \varphi < 60^\circ)$.

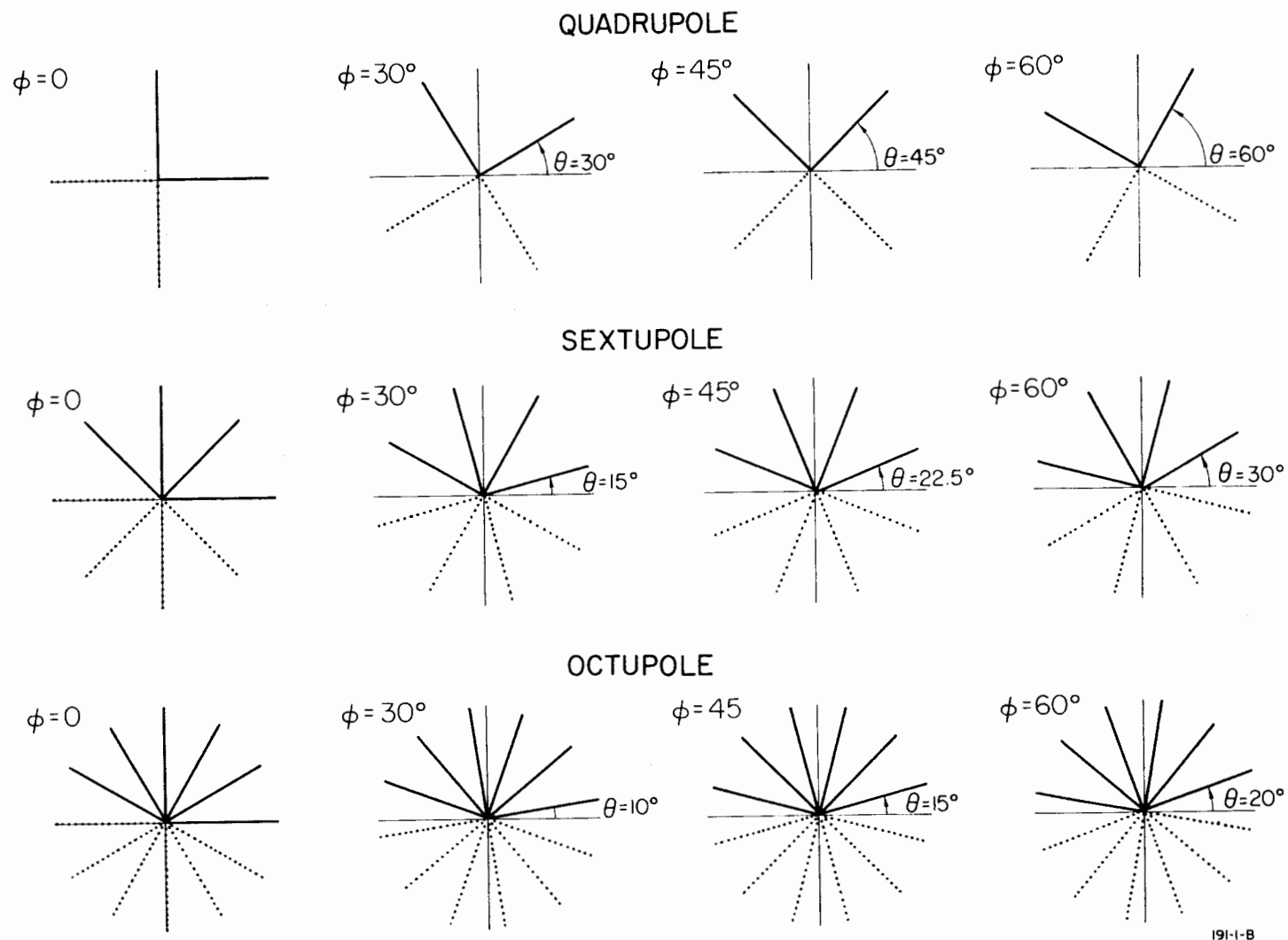


TABLE I. ANGULAR POSITION OF ZERO INTENSITY LINES

F. Applications

One of the most interesting applications of this light-scattering effect was that proposed by R. M. Johnson and which is described in Section III.A above. The vial with the polarizer and analyzer is mounted in a small carriage which can be moved along the Z axis of the magnet. With this device the "magnetic center line" can be measured. A typical measuring setup in a quadrupole magnet is shown in Fig. 13.

Figure 14 shows a measuring setup⁸ for aligning a quadrupole triplet collinearly for the accelerator with an accuracy of 0.001-inch. Here, to align the triplet magnetically, the center detector is inserted in quadrupole number 3 and the magnet is energized to its normal operating current. The telescope is then focused on the vial and the vial moved back and forth inside the cavity until the telescope is aligned along the magnetic center line of the quadrupole. This establishes the center line through all the magnets. As the alignment progresses, in order to assure that the telescope has not moved, a target is placed on the wall directly behind the magnet apertures, and once the center detector has been removed from the third quadrupole, the telescope is referenced to this target.

The center detector is now placed in quadrupole number 1. The vial is moved to the midpoint of the magnet and the location of the magnetic center is observed. The magnetic center at the midpoint of the quadrupole must be within 0.001-inch of the magnetic center line from the third quadrupole. Adjustments are now made to move the magnet until its magnetic center coincides with this magnetic center line as referenced to the alignment telescope. The vial is then moved near either end of the pole faces to determine whether or not the magnetic field is perpendicular to the center line.

When quadrupole number 1 is correctly aligned, the center detector is removed and placed in quadrupole number 2. The magnet will be energized and the same procedure will be used as in quadrupole number 1;

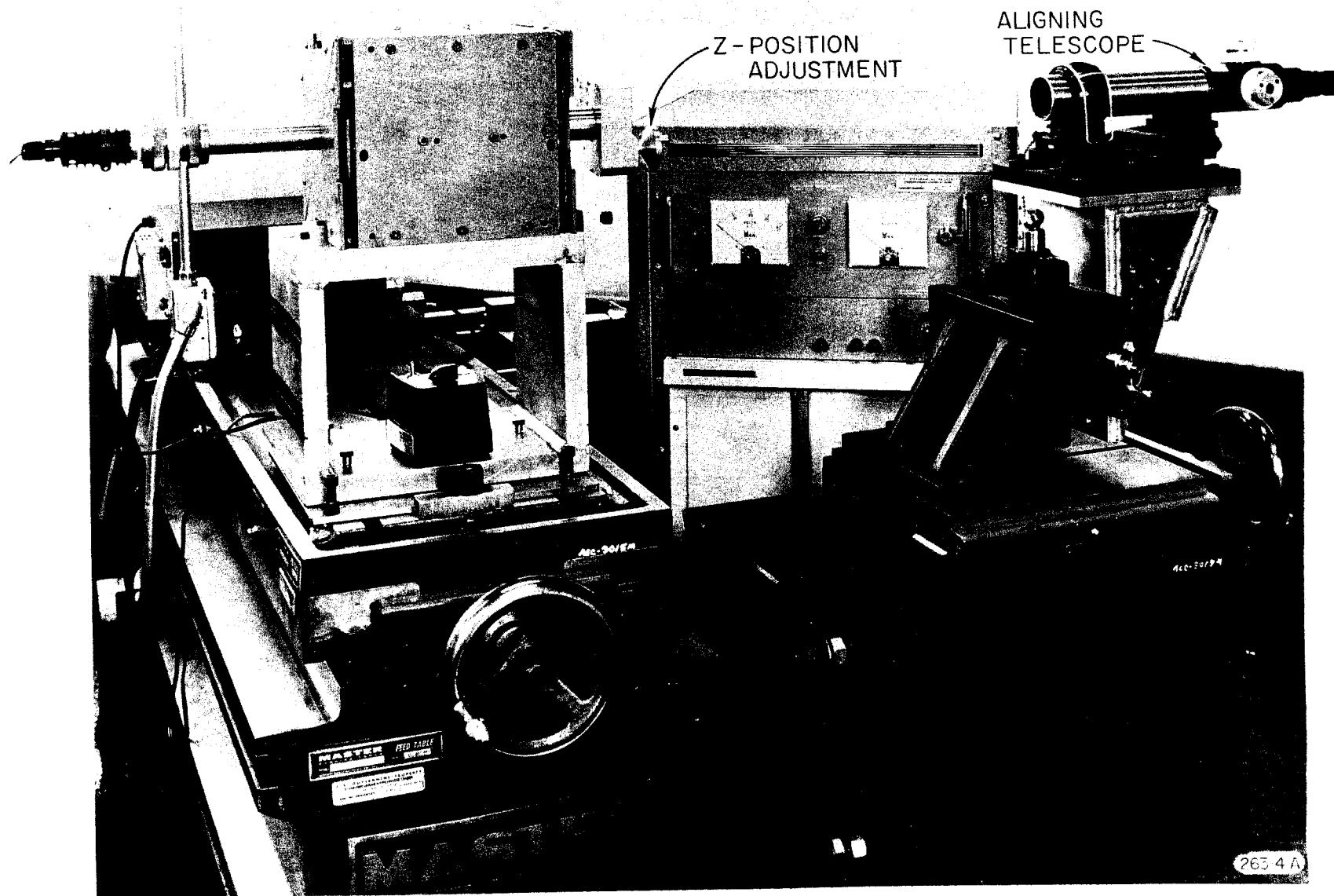
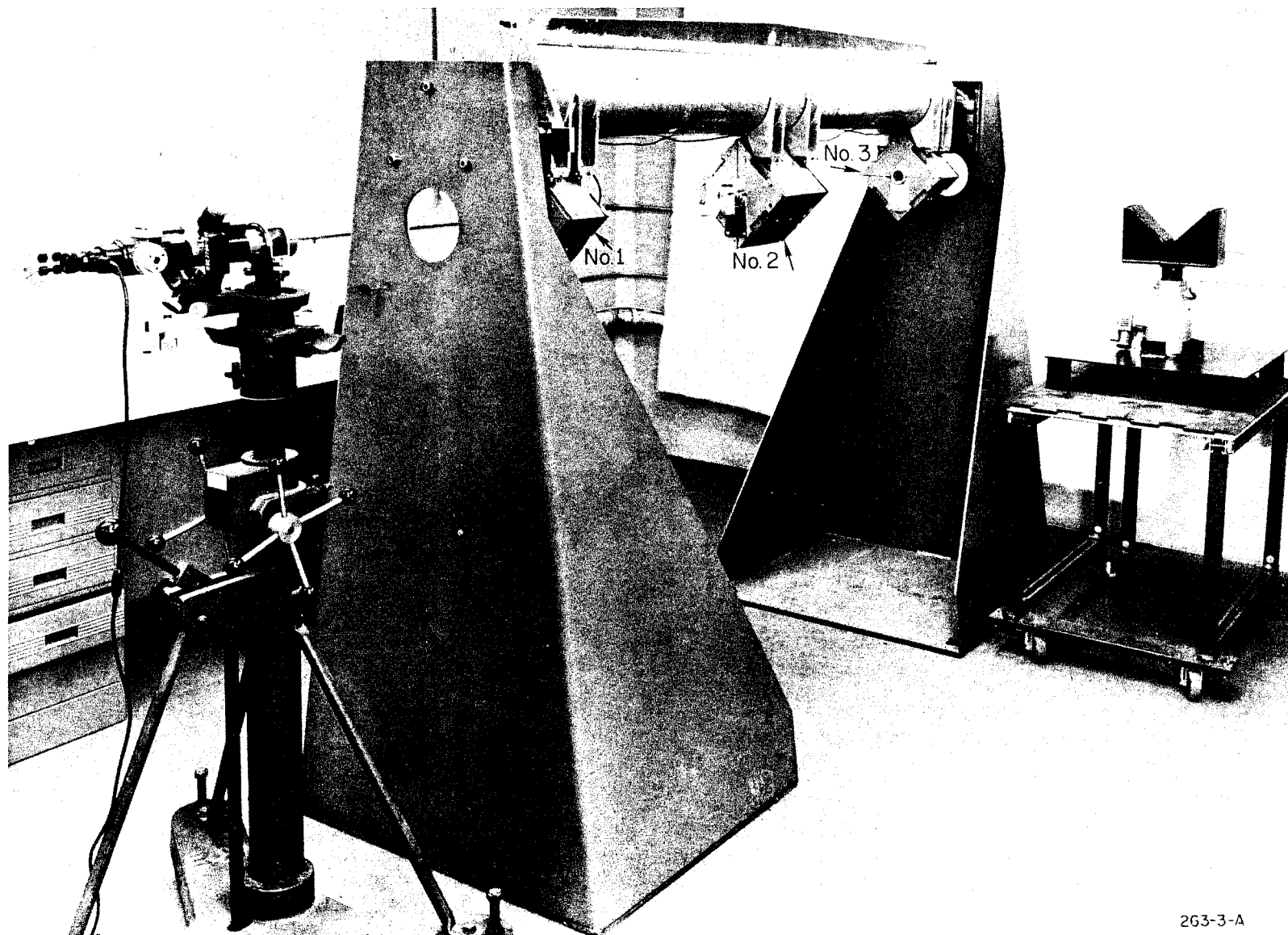


FIG. 13--Magnetic center location setup for a quadrupole magnet.



263-3-A

FIG. 14--Experimental setup for quadrupole alignment.

that is, the magnetic center of the magnet is adjusted to within 0.001 inch of the triplet's magnetic center line. By use of this method, any set of quadrupole magnets may be aligned collinearly to an accuracy of ± 0.001 inch. Figure 15 shows the required accessories for the triplet alignment.

Using the orientation of the dark cross, one can use this device to find the relation between the magnetic and mechanical axes in a quadrupole. Because of the unclear center portion, this method probably cannot be used for center location in higher poles.

IV. MEASUREMENT OF THE EFFECTIVE LENGTH IN MULTIPOLES

The action of a transverse magnetic field on a particle beam can be characterized by the integral

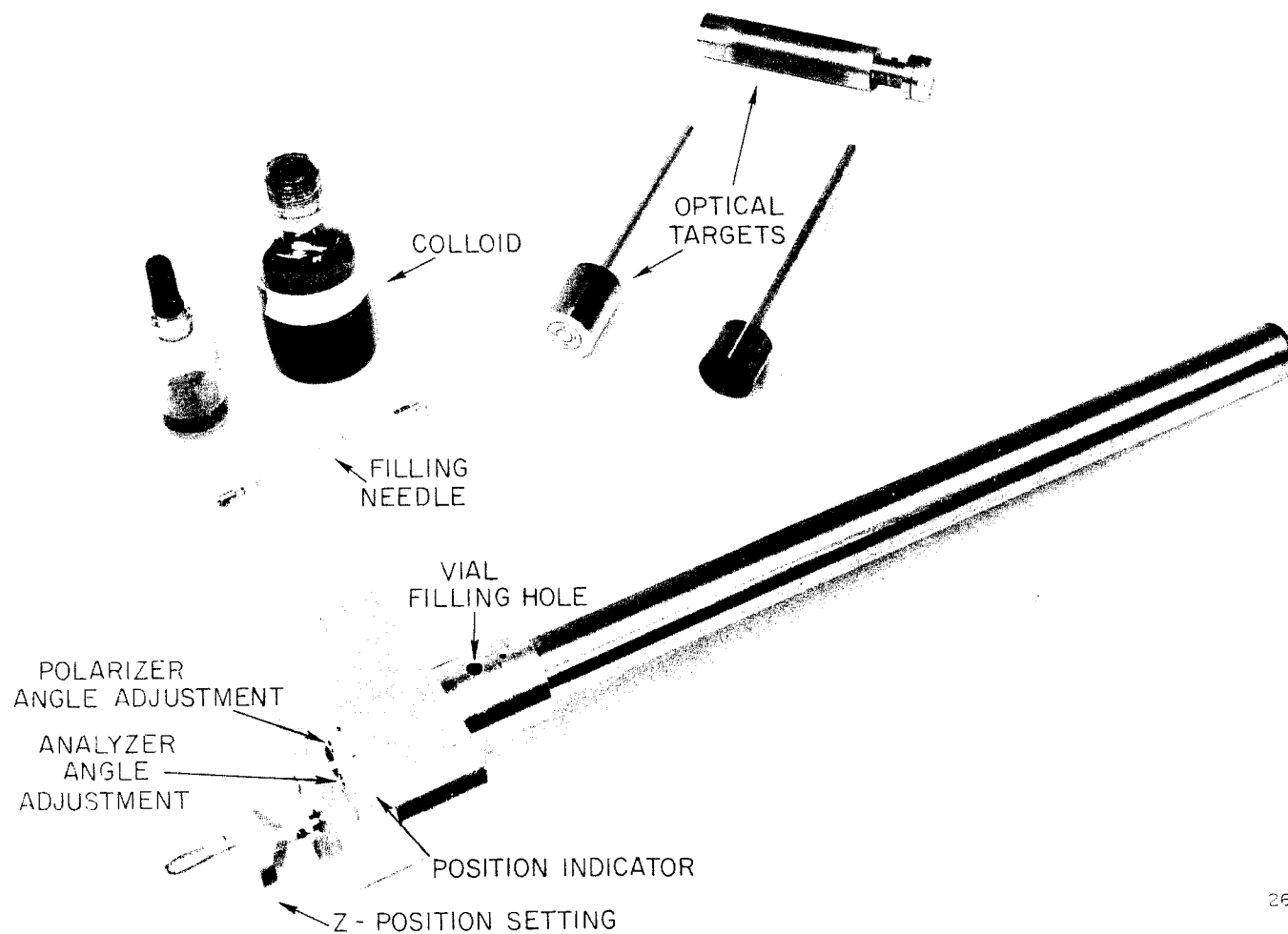
$$\int_{-\infty}^{\infty} B_r(r, z) dz$$

where the line integral is taken along the particle trajectory in the magnet system, and $B_r(r, z)$ is the magnitude of the transverse field component at a distance r from the center line (Oz) of the multipole field.

It is also very useful, especially for magneto-optical calculations, to define equivalent lengths for the multipole field components in a magnet system. Using the analog to the definition of the equivalent length in a dipole field,

$$L_1 = \frac{1}{B_0} \int_{-\infty}^{\infty} B(z) dz$$

one can define the effective length of the quadrupole, sextupole, and



263-L-A

FIG. 15--Detailed photo of magnetic center location.

octupole fields as

$$L_2 = \frac{1}{\frac{\partial B}{\partial r}(0,r)} \int_{-\infty}^{\infty} \frac{\partial B(z,r)}{\partial r} dz$$

$$L_3 = \frac{1}{\frac{\partial^2 B}{\partial r^2}(0,r)} \int_{-\infty}^{\infty} \frac{\partial^2 B(z,r)}{\partial r^2} dz$$

and

$$L_4 = \frac{1}{\frac{\partial^3 B}{\partial r^3}(0,r)} \int_{-\infty}^{\infty} \frac{\partial^3 B(z,r)}{\partial r^3} dz$$

One can simply show that there exist relations between L_1 eff, L_2 eff, L_3 eff, and L_4 eff. For example, the relation between L_1 eff and L_2 eff can be obtained⁹ from the following formula:

$$\begin{aligned} \frac{\partial L_1(r)}{\partial r} &= \frac{1}{B(0,r)} \int_{-\infty}^{\infty} \frac{\partial B(z,r)}{\partial r} dz - \frac{\frac{\partial B}{\partial r}(0,r)}{B^2(0,r)} \int_{-\infty}^{\infty} B(z,r) dz \\ &= \frac{\frac{\partial B}{\partial r}(0,r)}{B(0,r)} \left[\frac{\int_{-\infty}^{\infty} \frac{\partial B}{\partial r}(z,r) dz}{\frac{\partial B}{\partial r}(0,r)} - \frac{\int_{-\infty}^{\infty} B(z,r) dz}{B(0,r)} \right] \\ &= \frac{1}{r} [L_2(r) - L_1(r)] \end{aligned}$$

Then

$$L_2(r) = L_1(r) + r \frac{\partial L_1(r)}{\partial r}$$

Similarly, using the general relation

$$L_n(r) = L_{(n-1)}(r) + r \frac{\partial L_n(r)}{\partial r}$$

we get

$$L_3(r) = L_1 + 3r \frac{\partial L_1}{\partial r} + r^2 \frac{\partial^2 L_1}{\partial r^2}$$

$$L_4(r) = L_1 + 7r \frac{\partial L_1}{\partial r} + 6r^2 \frac{\partial^2 L_1}{\partial r^2} + r^3 \frac{\partial^3 L_1}{\partial r^3}$$

which means that the lengths of the sextupole and octupole field are calculable when the length of the dipole field and its first, second, and third derivatives are known.

The effective length of a quadrupole is one of its most important characteristics because it is used in the matrix element when calculating the beam dynamics in a magnetic lens system. In general, the effective length is a function of the radial position r from the magnetic axis of the quadrupole. There are several methods of finding the effective length. One involves using normal mapping procedures, plotting the field at a point r as a function of the axial position z for

$-\infty < z < \infty$ and integrating the area under the curve from $-\infty$ to ∞ .

This area is then divided by the maximum field, and thus the effective length of the dipole field L_B as a function of radial position is obtained. From this, using the formula

$$L_2(r) = L_1(r) + r \frac{\partial L_1(r)}{\partial r}$$

the length of the quadrupole field L_2 is calculable.

A second and easier method of effective length determination involves the use of four coils rotating on a single shaft¹⁰ (see Fig. 16). Two of the coils are long compared to the field while two are located in the central field of the magnet. The outputs from the long and short coils add in a quadrupole field but exactly cancel in a dipole field. The total output sinusoidal wave from the long coils is divided down on a precision potentiometer and compared with the total output sinusoidal wave from the short coils. The phase of the outputs is exactly the same because the long and short coils are built in the same plane. The two signals are thus compared until the divider potentiometer is set for complete cancellation of signals. Cancellation is facilitated by inversion of one signal with respect to the other, so that when the signals are equal they appear as a null. Then, measuring the ratio of the induced voltages and knowing the coil dimensions, the effective length of the quadrupole field is calculable. In this way, accuracy of about 0.1% is assured.

Figure 17 shows the experimental setup to measure L_2 . The rotating coil with the brush assembly is shown in Fig. 18.

V. SPECTROSCOPY OF MULTIPOLES

A. Experimental Setup

One of the most important methods of evaluating a multipole magnet is the determination of the harmonic content of its field. In any practical multipole magnet there are some higher harmonic fields present, and these, if sufficiently large, can affect the beam dynamics in the magnet. In some cases it is desirable to build magnets in which there is a large harmonic content in order to correct optical errors. One can use the information about the harmonics of a multipole magnet to design special pole faces^{11,12} or fringing fields for the magnetic multipoles. Using the symmetry conditions for the scalar magnetic potential, the harmonics contained in the field with quadrupole, sextupole, and octupole symmetry can be listed as shown in Table II.

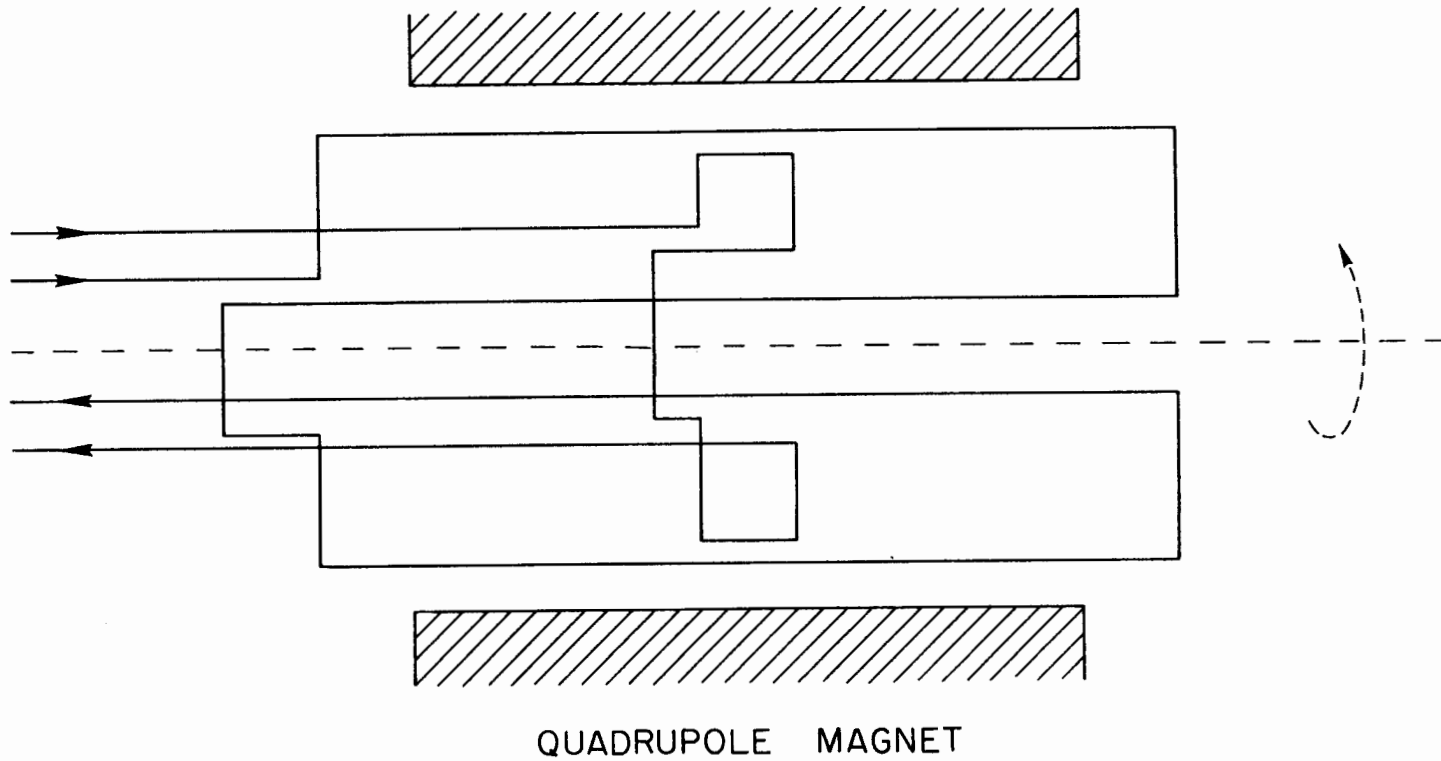


FIG.16 ROTATING COILS METHOD OF
EFFECTIVE LENGTH DETERMINATION

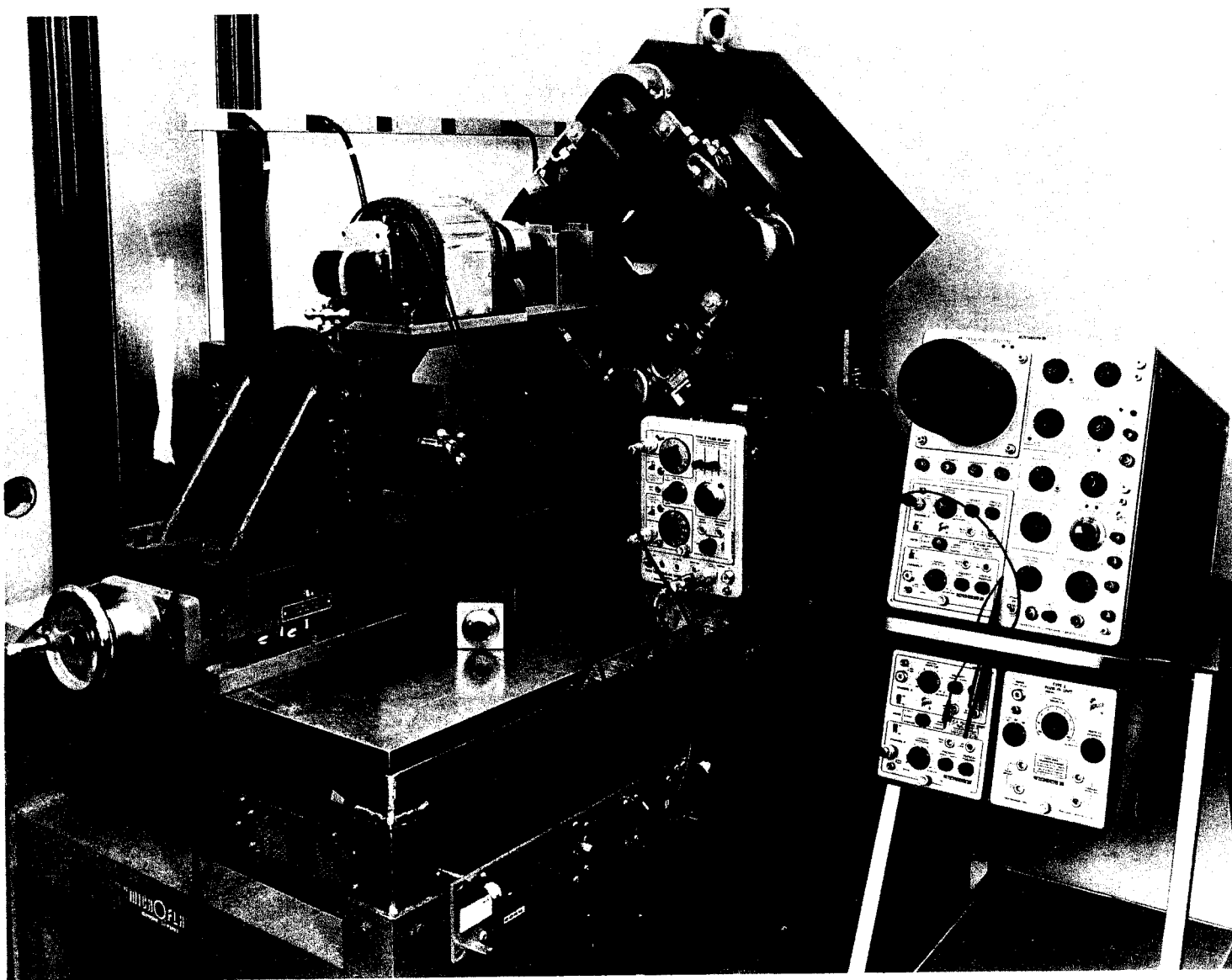


FIG. 17--Experimental setup for quadrupole effective length measurement.

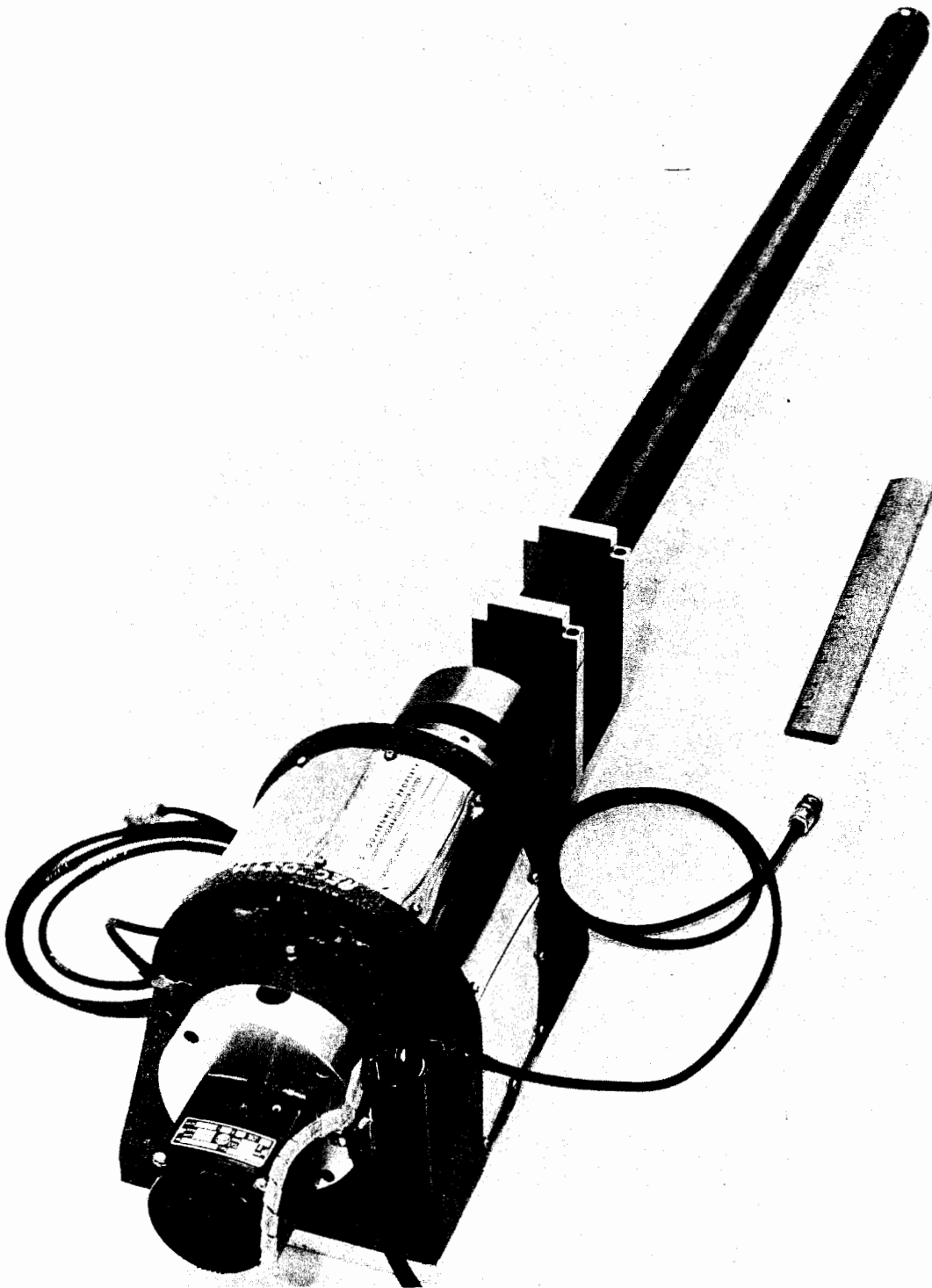


FIG. 18--Rotating coil assembly for effective length measurement.

TABLE II



The corresponding magnetic scalar potentials can be written as

$$u = \sum_{n=2,6,10,14,18, \dots} B_{2n}(\sin n\theta)r^n \quad \text{for quadrupole fields}$$

$$u = \sum_{n=3,9,15,21, \dots} B_{3n}(\sin n\theta)r^n \quad \text{for sextupole fields}$$

and

$$u = \sum_{n=4,12,20, \dots} B_{4n}(\cos n\theta)r^n \quad \text{for octupole fields.}$$

When the proper boundary conditions are satisfied, only one term remains in the summation. For example, in the case of the quadrupole only B_{22}

is the non-vanishing coefficient when the equipotential pole tip surfaces are in the form of equilateral hyperbolas in the X-Y coordinate system. By measuring $B_{2,6}$, $B_{2,10}$... in a quadrupole, one actually gets a measure of how well the pole faces approach the theoretical shape. In the case of pole saturation, because of the distortion of the ideal equipotential surfaces, the higher harmonic content increases. In a quadrupole, for example, $B_{2,6}$, $B_{2,10}$ will be non-vanishing at high field values even when at low field only B_{22} is not zero. If the symmetry conditions in a quadrupole are not completely satisfied, other coefficients such as B_{3n} , $n = 3, 9, 15, 21, \dots$, and B_{4n} , $n = 4, 12, 20 \dots$ will be present. Then, measuring B_{33} and B_{44} , one might draw conclusions about the quadrupole symmetry. One can analyze other multipoles in a similar manner.

To summarize, one might say that by measuring B_{mn} in a multipole (mn), where $n = m, m+2n, m+4n, \dots$, one gets a measure of how well the actual multipole approaches the theoretical multipole with ideal boundary conditions, and by measuring $B_{m'n'}$ where $m' = m+1, m+2, \dots$, $n' = m+1, (m+1)+2n', (m+2)+2n'$, one obtains a measurement of the symmetry of the multipole.

The existing harmonic content with all the amplitudes (B_{nm}) can be considered as the spectrum of the multipole. Naturally the amplitudes of the higher harmonics decrease rapidly with harmonic numbers. For example, in a quadrupole magnet, the pure quadrupole field (B_{22}) is much larger than other multipole field components, and some provision must be made to cancel or at least reduce the quadrupole field coefficient sufficiently so that its presence does not mask the other multipole coefficients.

To measure the higher harmonics one can use a special, asymmetrically wound, rotating coil which is designed to minimize the contribution due to the quadrupole field while enhancing the contributions from the other multipoles.¹³ The coil rotates at a fixed frequency synchronized to the A-C line. The output from the coil is Fourier-analyzed with a narrow bandwidth wave analyzer and the amplitude of each Fourier coefficient is noted. In this system, the Fourier coefficient corresponding to the frequency of rotation ω of the coil is the dipole field; the coefficient

corresponding to frequency 2ω is the quadrupole field; the coefficient of 3ω is the sextupole field, and so forth for higher fields. The rotating coil can be calibrated in multipole calibrating magnets of known field strength, or its response can be calculated for a given coil geometry.

A block diagram of such a harmonic analyzer system is shown in Fig. 19. Figure 20 shows the actual experimental setup used for analyzing a quadrupole magnet.

B. Coil Design and Calibration

The rotating coil used for harmonic analysis in a multipole field should be sensitive to the harmonic field components which are being measured. If a field component with large harmonic number is measured, it is desirable to suppress the coil sensitivity for the other harmonics, particularly when the corresponding fields are large in magnitude. For example, if one wants to measure B_{26} in a quadrupole field, it is necessary to minimize the coil response for B_{22} ; otherwise the small signal corresponding to B_{26} would be lost in the large signal background. With special coil design one can decrease the coil sensitivity for any one harmonic.

The coil response, the normalized voltage induced in the coil corresponding to the measured harmonic B_{nm} in a multipole $(2n)$, can be calculated or calibrated in a multipole magnet set at equal pole-field strength. In the following the coil response will be calculated for simple coil geometries used mostly for quadrupole harmonic analysis.

1. Flat Coil

The induced voltage in a single wire moving with an instantaneous velocity $\vec{v} = r\omega\vec{\theta}_0$ where $\omega = \frac{d\theta}{dt}$ in a multipole magnetic field can be expressed as

$$E' = \vec{B} \cdot \vec{\ell} \times \vec{v} = \vec{B} \cdot [\ell r \omega (\vec{Z}_0 \times \vec{\theta}_0)] = -\ell r \omega \vec{B} \cdot \vec{r}_0 = -\ell \omega r B_r$$

where ℓ is the length of the wire, $(\vec{\ell} = \ell \vec{Z}_0)$ and $\vec{B} = \mu_0 \vec{H}$.

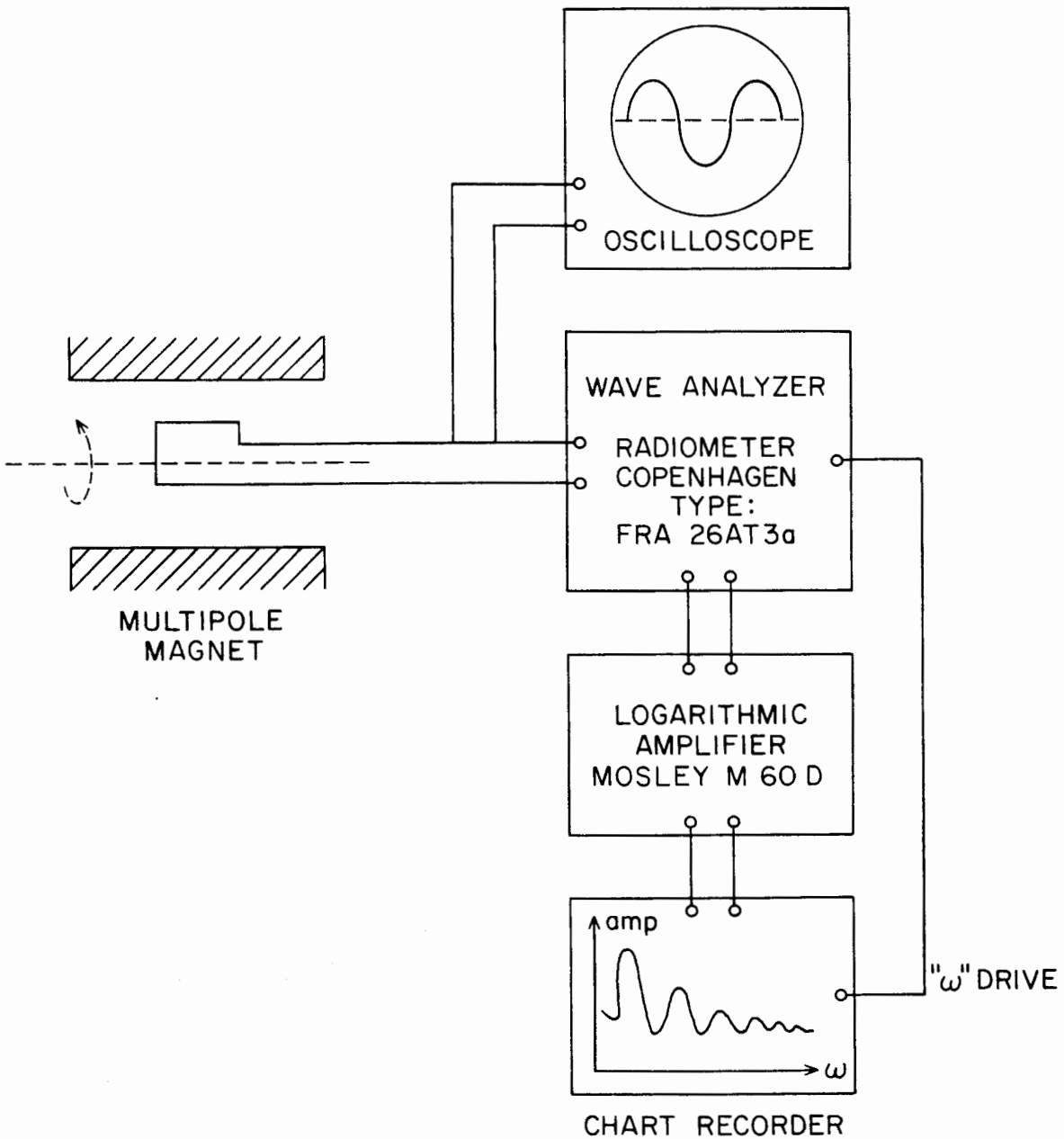


FIG.19 BLOCK DIAGRAM OF HARMONIC ANALYZER
FOR MULTIPOLE MAGNETIC FIELD SPECTROSCOPY

168-9-A

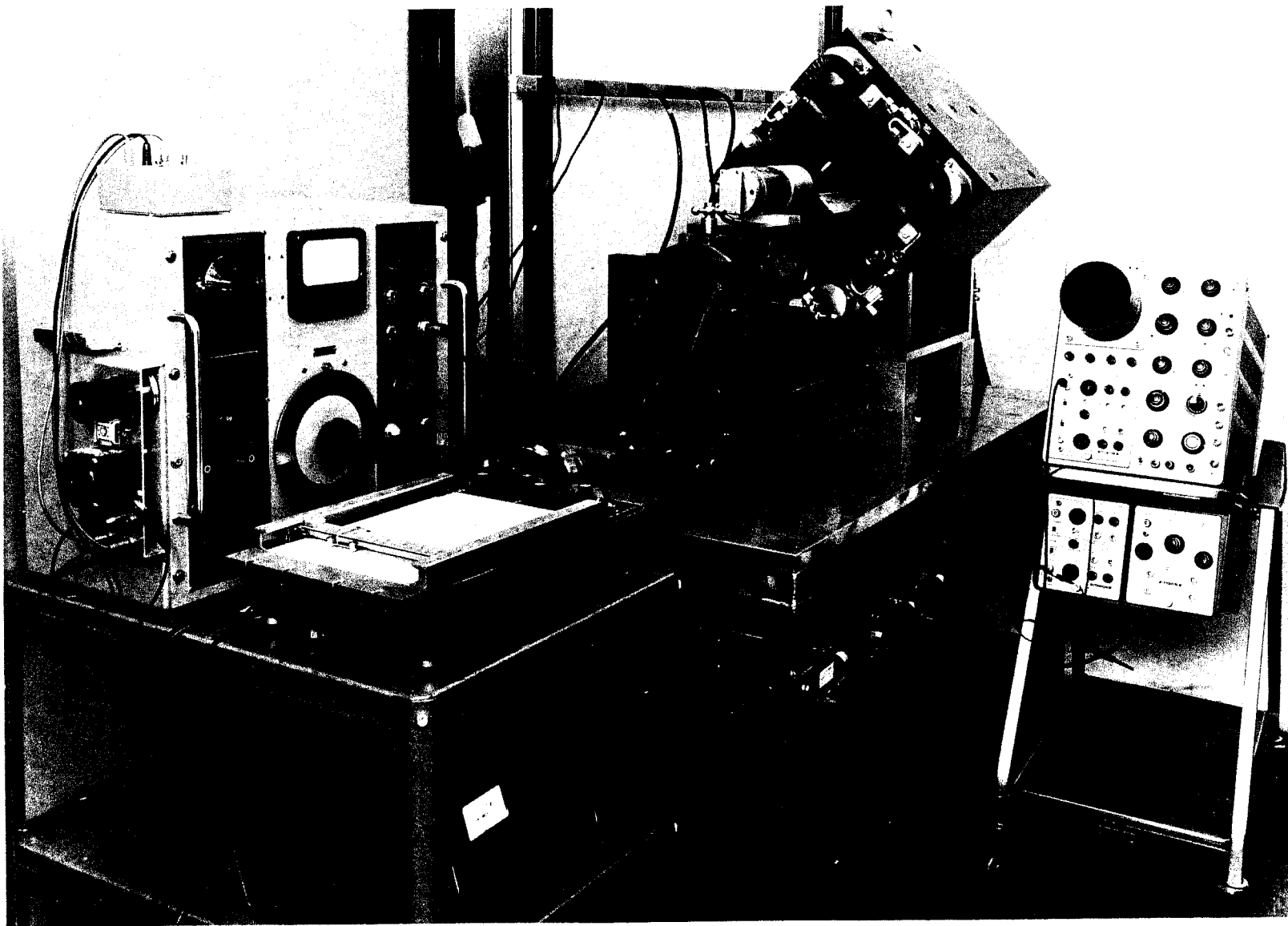


FIG. 20--Experimental setup for harmonic analysis in a quadrupole field.

However,

$$\vec{H} = -\nabla u = - \sum \left\{ nB_n r^{n-1} (\sin n\theta) \vec{r}_0 - nB_n r^{n-1} (\cos n\theta) \vec{\theta}_0 \right\}$$

and with this

$$E' = \mu_0 \ell \omega \sum nB_n r^n \sin n\theta$$

Let λ be the linear wire density, i.e., the number of turns per unit radial distance; then the induced voltage in the multi-wire system can be written as

$$E = \int_a^b \lambda E' dr = \mu_0 \ell \omega \lambda \sum_n B_n \sin(n\theta) \frac{n}{n+1} \left\{ b^{n+1} - a^{n+1} \right\}$$

In a symmetrical flat coil the return bundle is running in the opposite direction and located at $\theta = 180^\circ$. Therefore, the total voltage induced in the rotating coil is

$$E_c = E(a, b, \theta) - E(a, b, \theta + \pi)$$

$$= \mu_0 \ell \omega \lambda \sum B_n \frac{n}{n+1} \left(b^{n+1} - a^{n+1} \right) \left\{ \sin n\theta - (-1)^n \sin n\theta \right\}$$

From this it is obvious that

$$E_c = 0 \quad \text{for } n = 2, 4, \dots, 2m$$

This type of symmetric flat coil therefore cannot be used for quadrupoles, octupoles, etc.

2. Asymmetric Flat Coil

The next simplest coil configuration is the asymmetric flat coil, where the return bundle is located at the center of the axis of rotation and the coil has only one turn.

In this case the induced voltage in a one-turn coil is

$$E_c = \mu_o \ell \omega \sum_n n B_n r^n \sin n\theta$$

but with $\theta = \omega t$ and $B_n = B_o \left(\frac{1}{a}\right)^{n-1}$, where a is the half-aperture size of the multipole, one obtains for the induced voltage in a dipole field

$$E_1 = \mu_o B_o \ell \omega r \sin \omega t$$

for the induced voltage in a quadrupole field

$$E_2 = \mu_o \frac{B_o}{a} \ell \omega r^2 \sin 2\omega t$$

and in a sextupole field

$$E_3 = \mu_o \frac{B_o}{a^2} \ell \omega r^3 \sin 3\omega t$$

To find the ratio of the induced voltages for the rotating asymmetrical coil in quadrupole, sextupole, and octupole fields with equal field intensity at the pole face, one must average the output voltage over a half-revolution of the coil. Thus

$$\langle E_1 \rangle = \frac{\mu_o \ell B_o r}{\pi} \int_0^\pi \sin(\omega t) d(\omega t) = - \frac{2r\ell B_o}{\pi}$$

and because

$$\int_0^{\pi} \sin(n\omega t) d(\omega t) = 2 \quad \text{for } n = 1, 2, 3 \dots$$

one gets

$$\langle E_n \rangle = - \frac{2r\ell B_0}{\pi} \left(\frac{r}{a} \right)^{n-1}$$

and the coil response for different harmonics is

$$\frac{\langle E_n \rangle}{\langle E_1 \rangle} = \left(\frac{r}{a} \right)^{n-1}$$

Figure 21 shows calculated and measured response curves for an asymmetric flat coil with $\left(\frac{r}{a} \right) = \frac{7}{16}$.

As mentioned earlier, the coil response can be measured with the harmonic analyzer system in different multipoles with equal half-apertures and field strength of the pole face. Such a coil response calibrating multipole magnet set is shown in Fig. 22. If the response of the measuring coil is known, then using the formula for the induced voltage, the field corresponding to any multipole content can be calculated.

3. Asymmetric Coil

W. H. Lamb calculated¹³ the induced voltage in a rotating asymmetric coil where two return bundles are used. The return bundles are located at an angle α from the main bundle so that $\theta = \theta - \alpha$ for one and $\theta' = \theta + \alpha$ for the other. Figure 23 shows the arrangement of the wire bundles on the rotating coil. The induced voltage in this coil is given as

$$E_n = \mu_0 \ell \omega \lambda \sum \frac{n}{n+1} \sin n\theta' \left[\left(r_{1a}^{n+1} - a^{n+1} \right) - \left(r_{1b}^{n+1} - b^{n+1} \right) 2 \cos n\theta' \right]$$

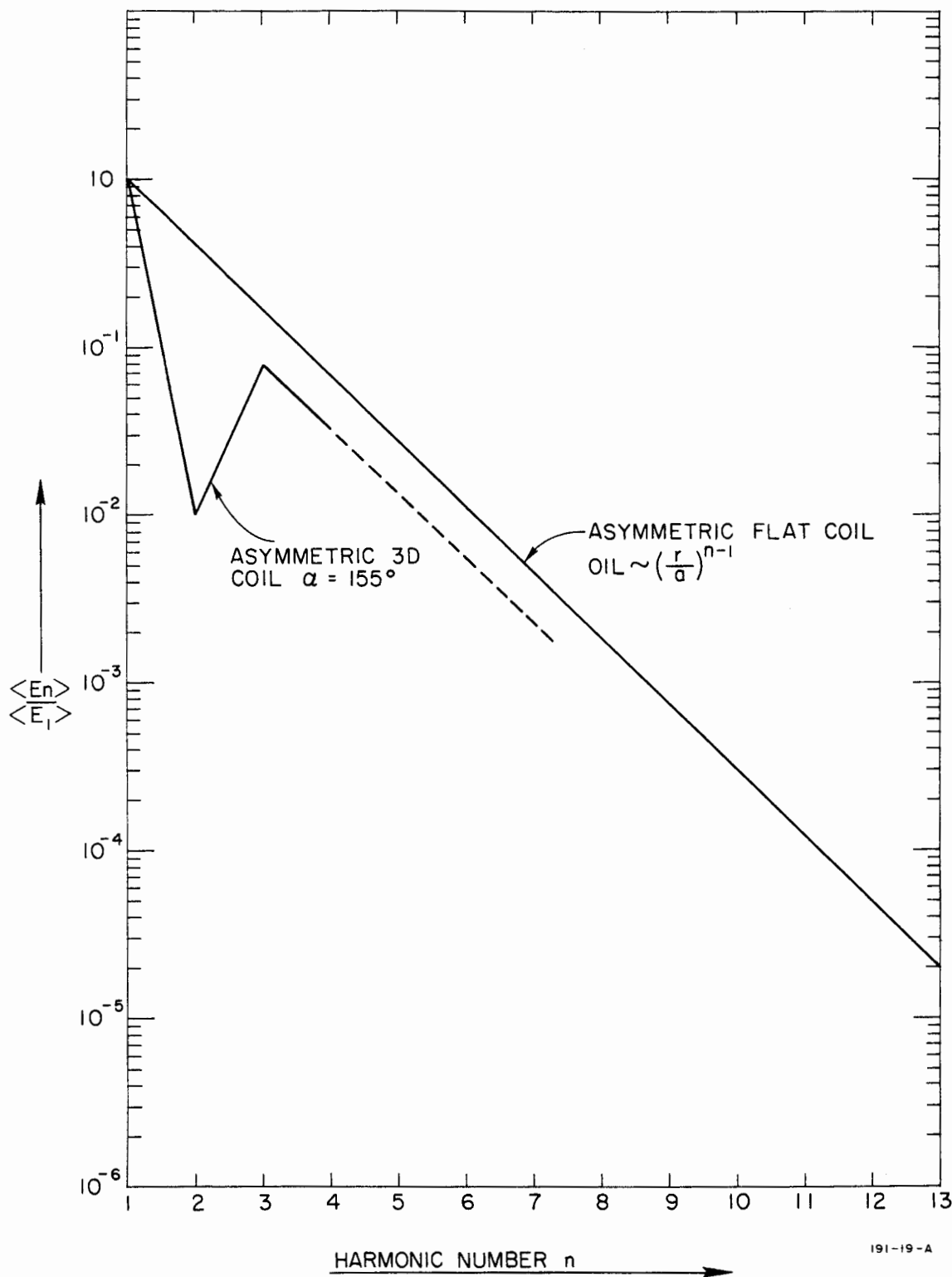


FIG. 21 - RESPONSE CURVE FOR THE ASYMMETRIC FLAT COIL

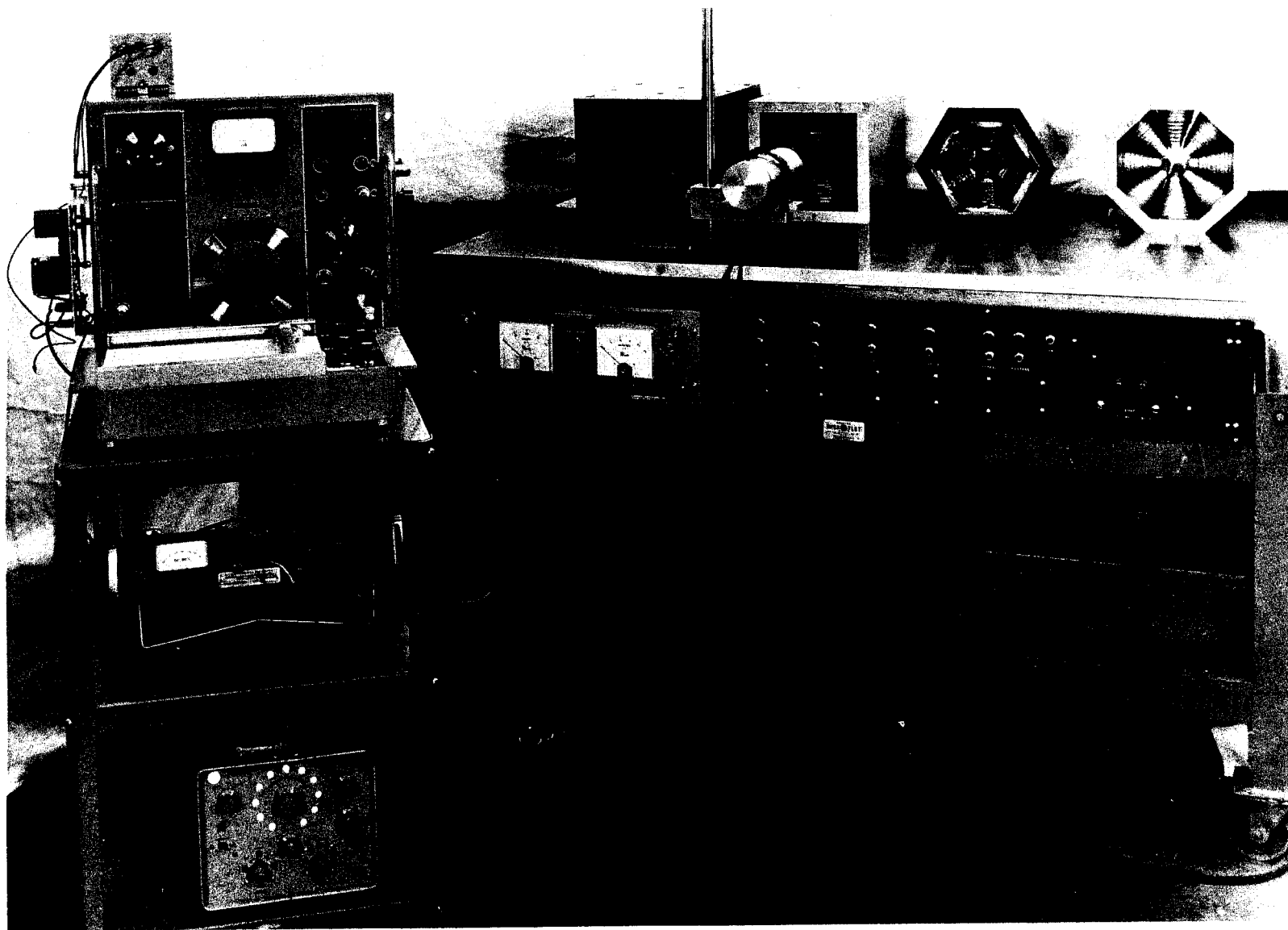
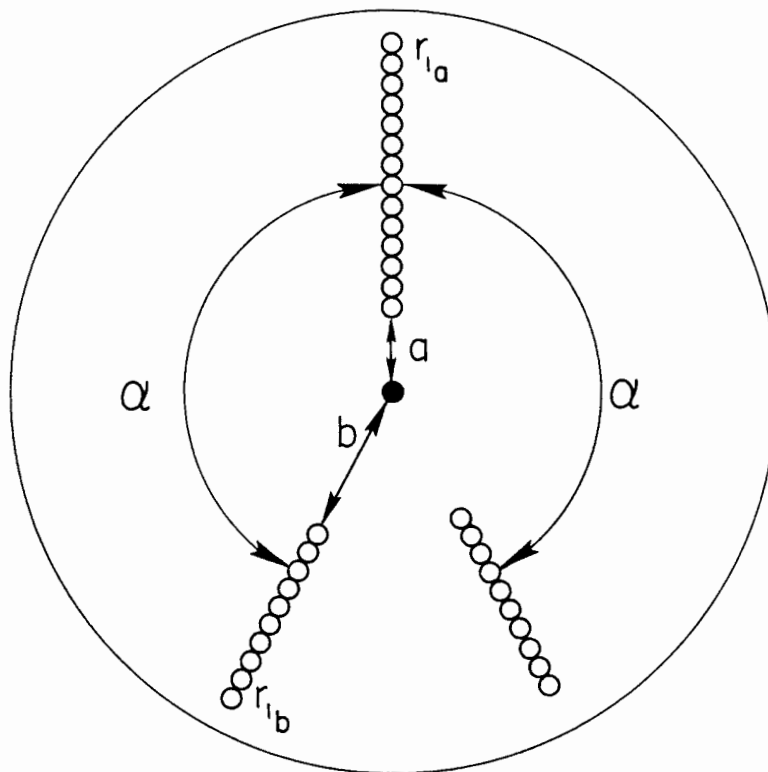


FIG. 22--Calibrating multipole magnets for rotating coil calibration
for quadrupole field spectroscopy.



191-6-A

FIG.23 - GEOMETRY OF COIL ARRANGEMENT
ON ROTATING ASYMMETRICAL COIL.

With this formula the coil response $\left\langle \frac{E_n}{E_1} \right\rangle$ can be calculated by a method similar to that demonstrated for the asymmetric flat coil. Using the formula for the induced voltage in an asymmetric rotating coil, it is possible to make the voltage response of the coil for the n-th harmonic vanish. For example, the condition that the voltage response is zero for B_{22} is such that

$$\left[\left(r_{1a}^3 - a^3 \right) - \left(b^3 - r_{1b}^3 \right) 2 \cos 2\alpha \right] = 0$$

Figure 21 shows the response characteristics of an asymmetric coil in magnetic multipole fields with equal field strength at the pole faces. The coil parameters are:

$$\begin{aligned} \alpha &= 155^\circ \\ a &= 2.77 \times 10^{-3} \text{m} \\ r_{1a} &= 10.9 \times 10^{-3} \text{m} \\ b &= 7.62 \times 10^{-3} \text{m} \\ r_{1b} &= 11.7 \times 10^{-3} \text{m} \end{aligned}$$

It can be seen from the response characteristics that the coil is more sensitive for measuring B_{33} than it is for B_{22} . This coil is particularly designed to measure the sextupole field in a quadrupole-sextupole magnet. Figure 24 shows a few of the coils which were used for multipole field measurements.

Table III summarizes the multipole field amplitudes which can be measured with the different coil geometry considered here.

C. Center Location with Rotating Coil

Using a rotating symmetrical or an asymmetrical coil, the center of a multipole can be located. The output signal is minimum when the axis of the coil coincides with the axis of the multipole. In a quadrupole it is desirable to use a symmetric flat coil because it does not respond to the quadrupole field. Figure 25 shows the amplitude of the first harmonic vs the vertical displacement in a quadrupole magnet. It can be



FIG. 24--Rotating coil configuration used in multipole field spectroscopy.

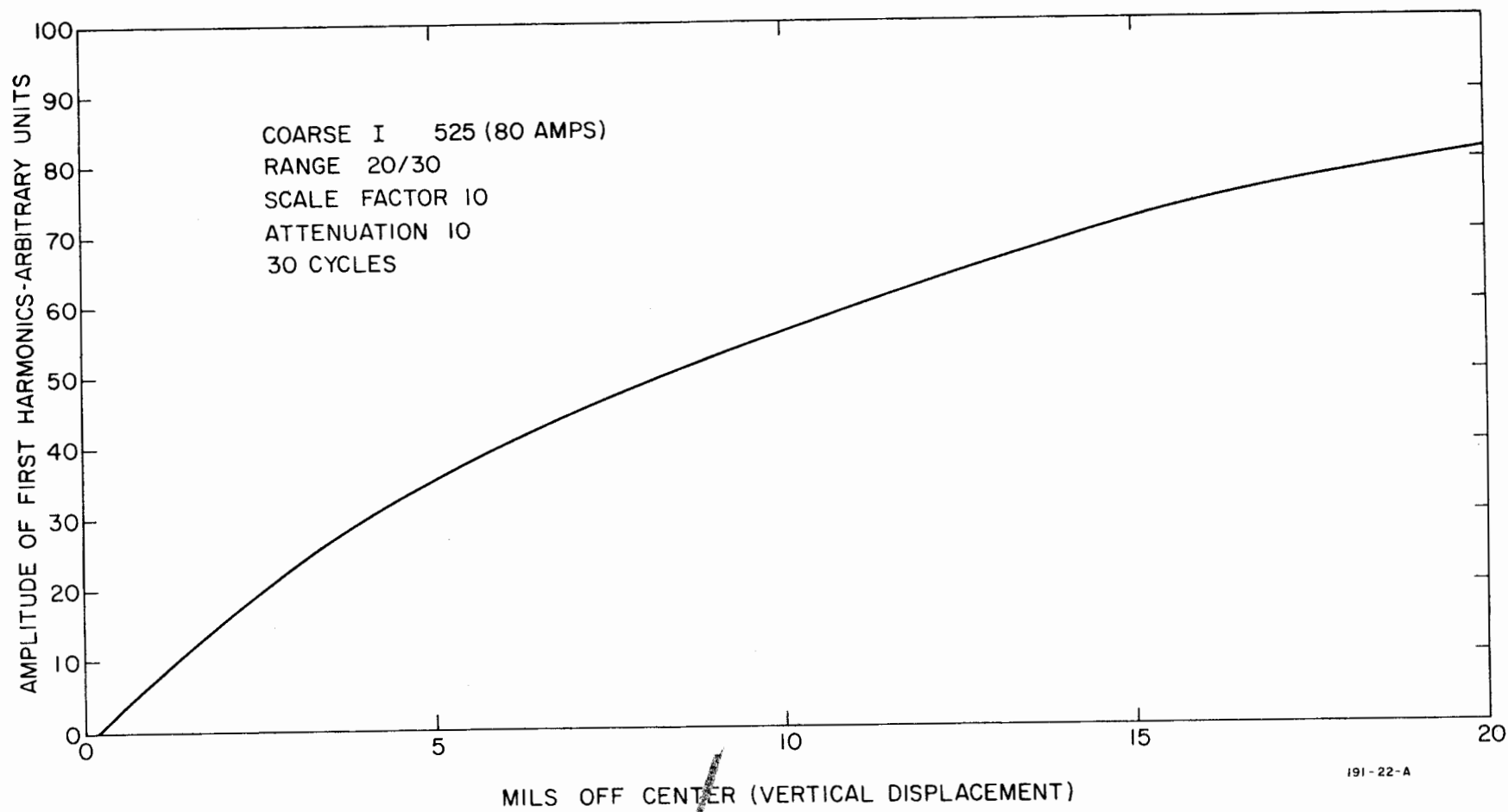


FIG. 25 - AMPLITUDE OF FIRST HARMONIC vs. DISPLACEMENT OFF CENTER

seen that with this method the center of the quadrupole can be located better than ± 1 mil. Any change in the field value at the pole face in a quadrupole will result in a shift in the position of the center. Figure 26a shows the change in the amplitude in the first harmonic as a function of the strength of the perturbation caused by an extra perturbing coil.

TABLE III

Multipole	Flat Coil	Flat Asymmetric Coil	Asymmetric Coil for Quadrupole
Dipole	$B_{11}, B_{13}, B_{15} \dots$	All	All
Quadrupole	0	All	Less sensitive for B_{22} than for $B_{2,6}, B_{2,10} \dots$
Sextupole	$B_{31}, B_{32}, B_{33} \dots$	All	All
Octupole	0	All	All
Decapole	$B_{51}, B_{52}, B_{53} \dots$	All	All

With this very sensitive measuring technique one can observe a change in the position of the magnetic center with increasing field. From this measurement one might estimate the change in symmetry due to the forces acting on the poles. In the case of an actual spectrum measurement in a multipole, one first centers the rotating coil by minimizing the first harmonic, then measures the amplitude of each harmonic. In a quadrupole field E_2 is independent of the position of coil; therefore, in a quadrupole field the meaningful normalized amplitudes are $\frac{E_3}{E_2}, \frac{E_4}{E_2}, \dots, \frac{E_n}{E_2}$. Similarly, in a sextupole field $\frac{E_2}{E_3}, \frac{E_4}{E_3}, \frac{E_5}{E_3}, \dots, \frac{E_n}{E_3}$ are the useful amplitudes.

D. Effective Length Measurement with Rotating Coil

Using the harmonic analyzer with a rotating pickup coil moving along the z-axis, one can measure the effective length of any multipole field. The selective amplification of the required multipole field induced signal makes it possible to measure the length of any harmonic field in a multipole.

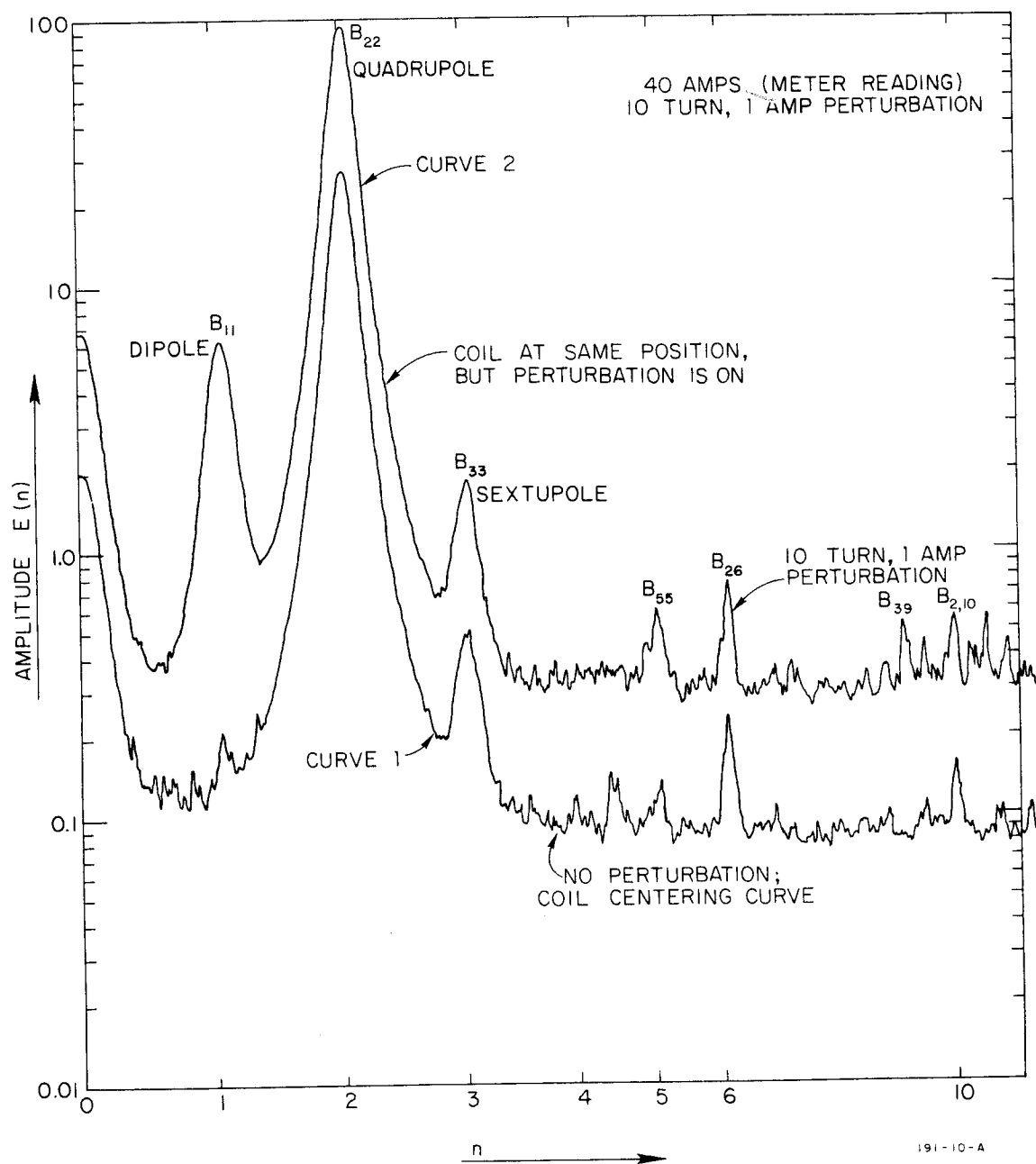


FIG. 26 a - EFFECT OF PERTURBATION ON QUADRUPOLE SPECTRUM

E. Effect of the Field Perturbation in Multipole Fields

The field configuration in a multipole is perturbed when the field strengths at the pole faces are different in absolute values or when the shapes of the pole faces are not identical. In both cases the symmetry conditions are not satisfied and higher-order multipole field amplitudes do not vanish. When one of the pole faces has a different shape, higher harmonics belonging to the same symmetry condition will have non-zero values. Figure 26a shows a quadrupole spectrum without perturbation (curve 1) and in the same position but with perturbation (10-turn coil excited by 1-ampere current) on one of the pole faces (curve 2). One of the obvious effects of this perturbation is the change in the location of the quadrupole's magnetic center. The first harmonic (B_{11}) has increased appreciably, showing that the center moved. The spectrum of the quadrupole after the coil was recentered is shown in Fig. 26b. Comparing this perturbed spectrum with the spectrum without perturbation, one can see the new higher harmonic content (B_{55} , B_{77} , B_{88} , B_{39} , B_{11}) which is the result of the lack of symmetry in the quadrupole.

Figures 27a, 27b, and 27c show the perturbation effect of a ferromagnetic wire placed on one of the pole faces in the quadrupole and suspended near the pole face. Figure 27a shows the unperturbed spectrum taken by a rotating coil which is centered on the magnetic axis. In Fig. 27b, the spectrum is shown when a 1-mm-diameter steel wire is placed along the pole face and the coil again centered. Figure 27c shows the spectrum taken by the centered coil when the wire is suspended in the quadrupole field. Comparing these spectrums, one can observe that the new higher harmonics appeared due to the perturbation (B_{44} , B_{77} , B_{99}) which spoiled the symmetry, and other harmonics with quadrupole symmetry (B_{26}) increased in amplitude because the "ideal" boundary surfaces were changed.

Generally then, a change in the boundary conditions changes the symmetry in the multipoles. This property of the multipoles can be useful in designing, for example, a quadrupole-sextupole magnet in which the relatively large sextupole content might correct the aberration of the quadrupole pairs in a certain momentum region.

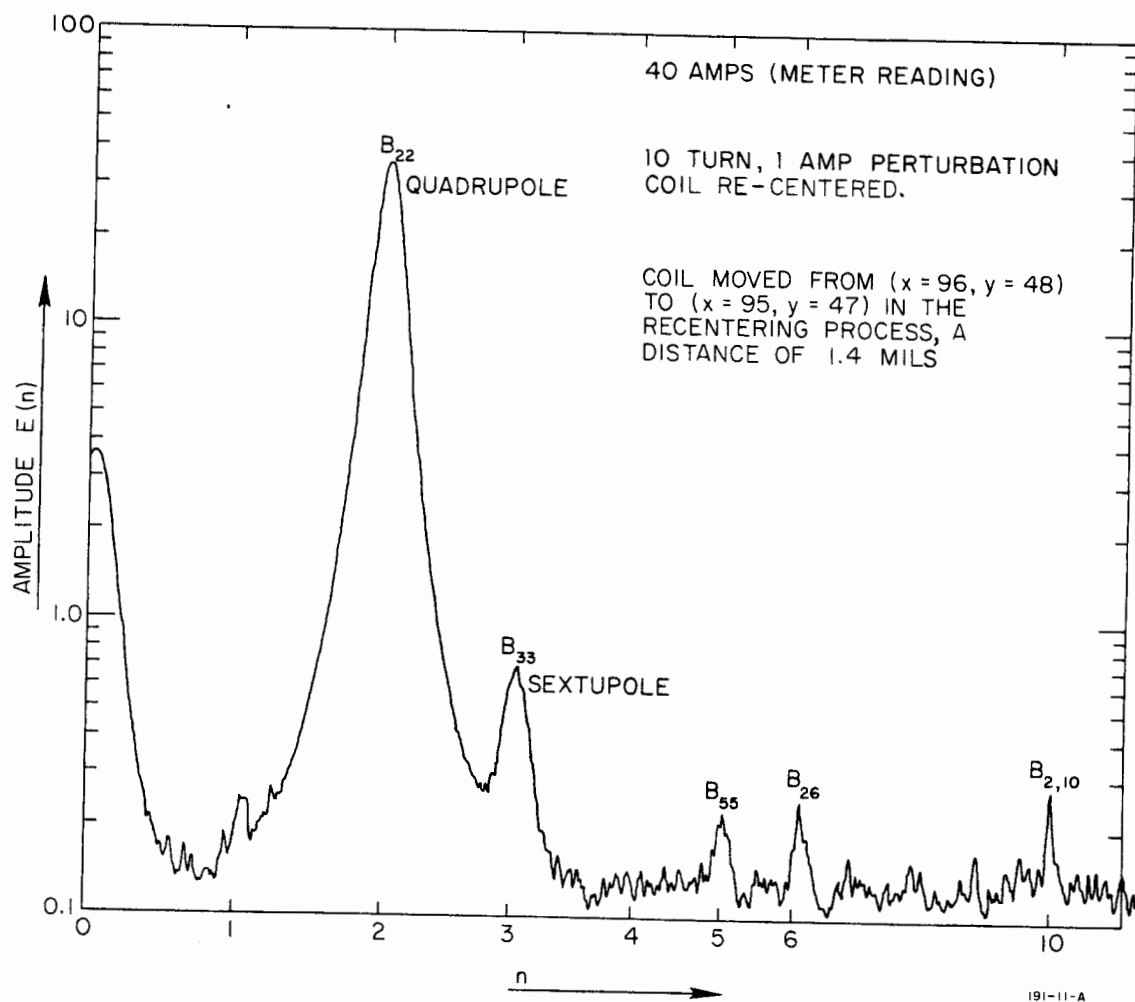


FIG. 26 b - EFFECT OF PERTURBATION ON QUADRUPOLE SPECTRUM

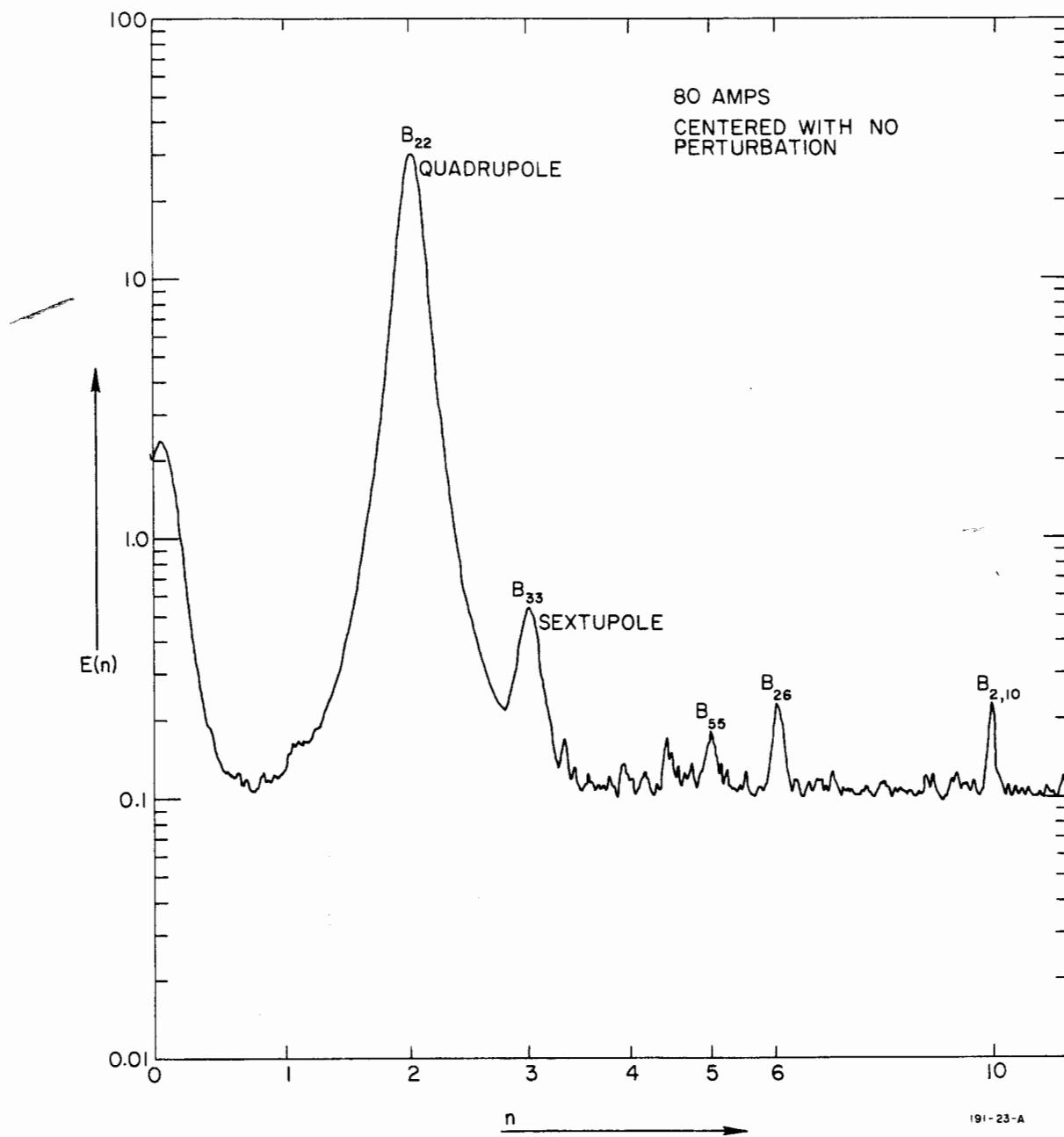


FIG. 27a - EFFECT OF POLE FACE PERTURBATION ON A QUADRUPOLE SPECTRUM

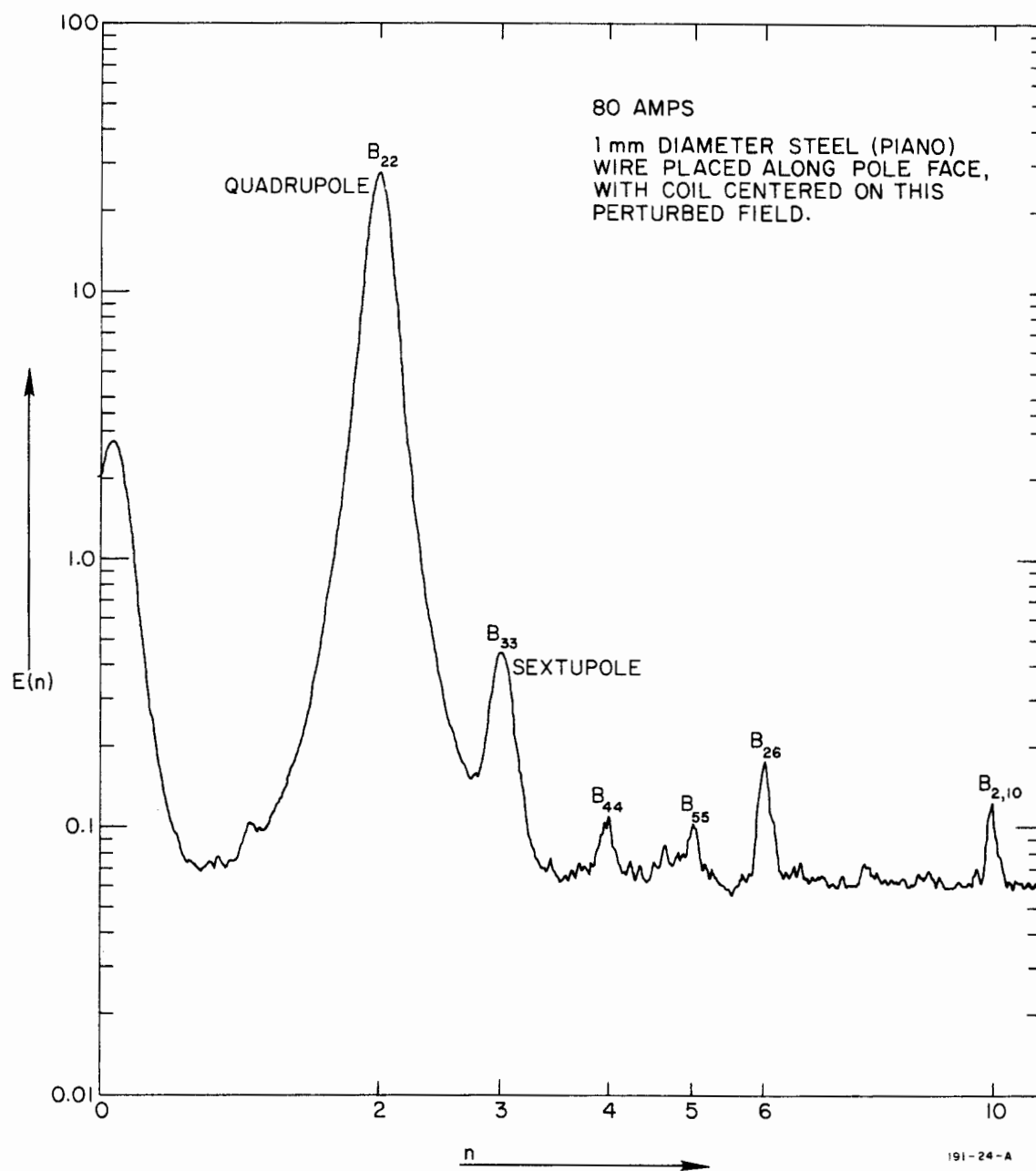


FIG. 27 b - EFFECT OF POLE FACE PERTURBATION ON QUADRUPOLE SPECTRUM

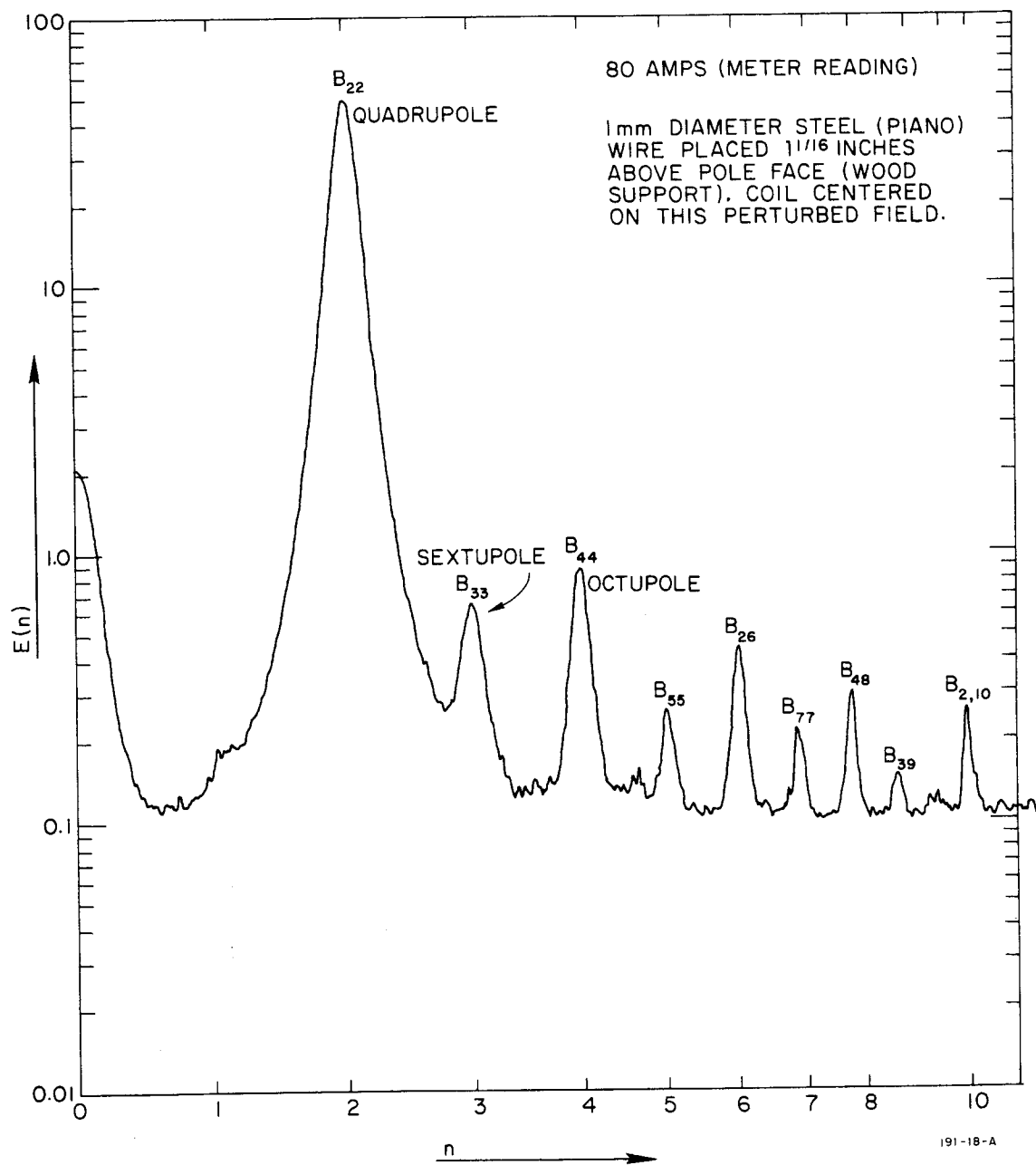


FIG. 27c - EFFECT OF POLE FACE PERTURBATION ON QUADRUPOLE SPECTRUM

VI. GRADIENT MEASUREMENT IN MULTIPOLES

One of the best methods of specifying the quality of a given quadrupole is the constancy of the gradient $\partial B_r / \partial r$ over the aperture of the magnet. Because the direction of the field vector is a function of azimuthal angle in the aperture, the gradient is usually determined along the two axes, one principal and one secondary. The simplest method of examining the deviation of the gradient along an axis is by normalizing the gradient at a point to the gradient at the center of the magnet. Thus referring to the axis X , the gradient deviation would be expressed as a function of X as

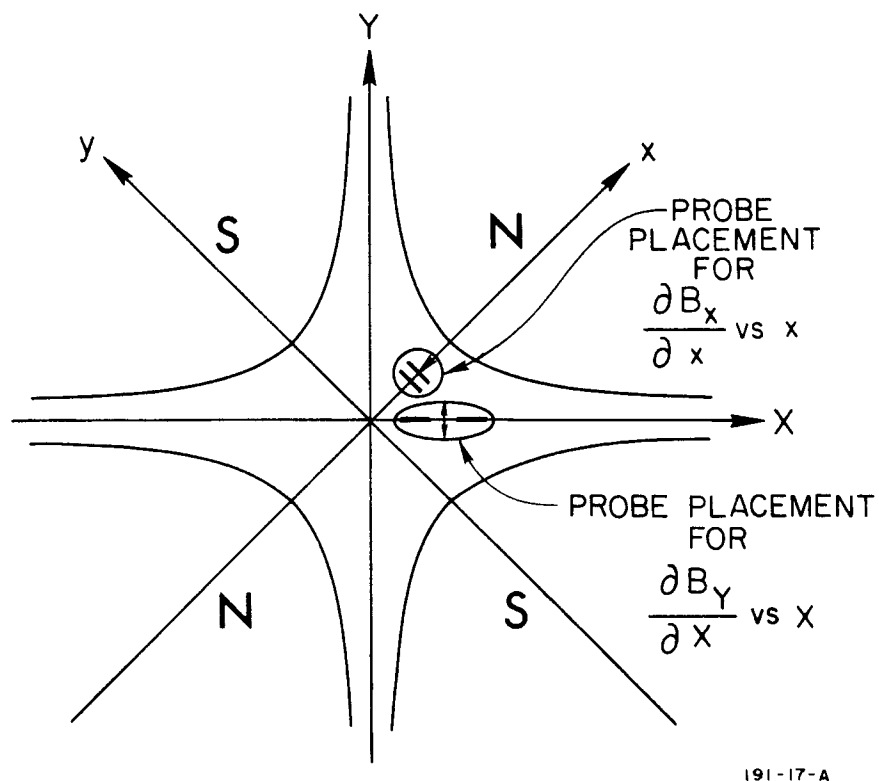
$$\frac{\partial B_Y}{\partial X} \bigg/ \left(\frac{\partial B_Y}{\partial X} \right)_{X=0},$$

and along the axis x the equivalent expression would be

$$\frac{\partial B_x}{\partial x} \bigg/ \left(\frac{\partial B_x}{\partial x} \right)_{x=0}.$$

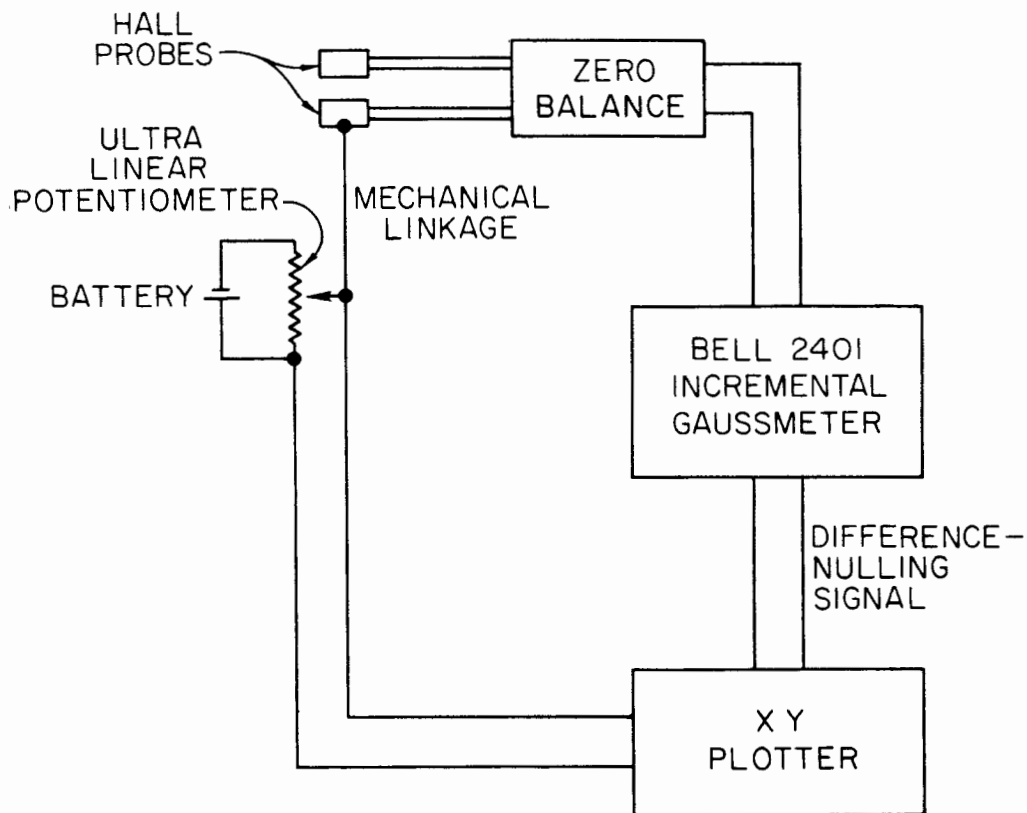
Among the methods available to measure these quantities, one of the easiest to use is a pair of closely matched linear hall probes mounted so that they are spaced δY for the measurement of the gradient versus displacement in X and Δx for the measurement of the gradient versus displacement in x (see Fig. 28).

Since the procedure for making the measurement is essentially similar along the two axes, this description will be about the measurement in X only. Figure 29 shows the system instrumentation. The hall probes are calibrated first so that they generate an equal signal when in an equal field. The difference between the hall probes output is determined for the case when the probes are at the center of the magnet, and this difference signal is then nulled with an external voltage. Next, the probes as a unit are displaced along the principal axis and the change in difference versus position from the center is recorded. This



191-17-A

FIG. 28 - PROBE ARRANGEMENT FOR MAKING GRADIENT MEASUREMENTS IN QUADRUPOLES



191-8-A

FIG. 29 - SYSTEM LAYOUT FOR MAKING GRADIENT MEASUREMENTS

operation yields the quantity $\partial B/\partial x - \partial B/\partial x|_{x=0}$. Normalizing this to the gradient at the center of the aperture $\partial B/\partial x|_{x=0}$, one obtains

$$\frac{\delta \left(\frac{\partial B}{\partial x} \right)}{\frac{\partial B}{\partial x}|_{x=0}}$$

the nonlinearity of the gradient over the aperture. In an ideal quadrupole magnet this would be zero for all values of x . In a practical quadrupole there is some nonlinearity caused by the factors mentioned earlier in Section II.B. Referring to that discussion, one can construct what nonlinearity of gradient will result from the truncation of the poles and from various misalignments and asymmetries in the construction.

The ways that various multipole fields will scale as a function of the radial position r are as follows. The dipole field is of course constant; the quadrupole field increases linearly with r/R as one moves from the center to the aperture radius R . The sextupole goes as $(r/R)^2$ and the other multipoles can be seen to scale as

$$\text{octupole,} \quad \left(\frac{r}{R} \right)^3$$

$$\text{decapole,} \quad \left(\frac{r}{R} \right)^4$$

$$\text{duodecapole,} \quad \left(\frac{r}{R} \right)^5$$

$$\text{n-th pole field,} \quad \left(\frac{r}{R} \right)^{\frac{n}{2}-1}$$

If the observed higher pole magnitude is normalized to the quadrupole magnitude, the resultant curve of a field will look like

$$\frac{\left(\frac{r}{R} \right)^{\frac{n}{2}-1}}{\left(\frac{r}{R} \right)^1} = \left(\frac{r}{R} \right)^{\frac{n}{2}-2}$$

Therefore, if a sextupole field is present in the measured field it will show up as a straight line with constant slope. The quadrupole contribution of course will be zero over the aperture. The octupole will be indicated by a field distribution that will be parabolic or proportional to r^2 , the decapole by an r^3 dependence, and the duodecapole by an r^4 dependence. Thus an examination of the gradient over the aperture will show immediately which higher multipoles are present. Of course, the higher multipoles are usually present in some combination rather than some pure perturbation; the field perturbation can be expressed as a polynomial as:

$$G = Ax^0 + Bx^1 + Cx^2 + Dx^3 \dots$$

where the coefficients are fractional parts of the field gradient caused by the presence of various multipoles. Figure 30 is a sketch of the expected gradient deviations caused by various pure perturbations.

VII. OPTICAL PROPERTIES OF MULTIPOLES¹⁴

This section will review briefly how the measured parameters of a multipole can be used to calculate the optical properties of the magnet.

It was shown earlier that the magnetic field distribution in a perfect quadrupole field can be derived from the magnetic scalar potential

$$u = -GXY$$

so that the field components of the field are

$$B_X = - \frac{\partial u}{\partial X} = GY$$

$$B_Y = - \frac{\partial u}{\partial Y} = GX$$

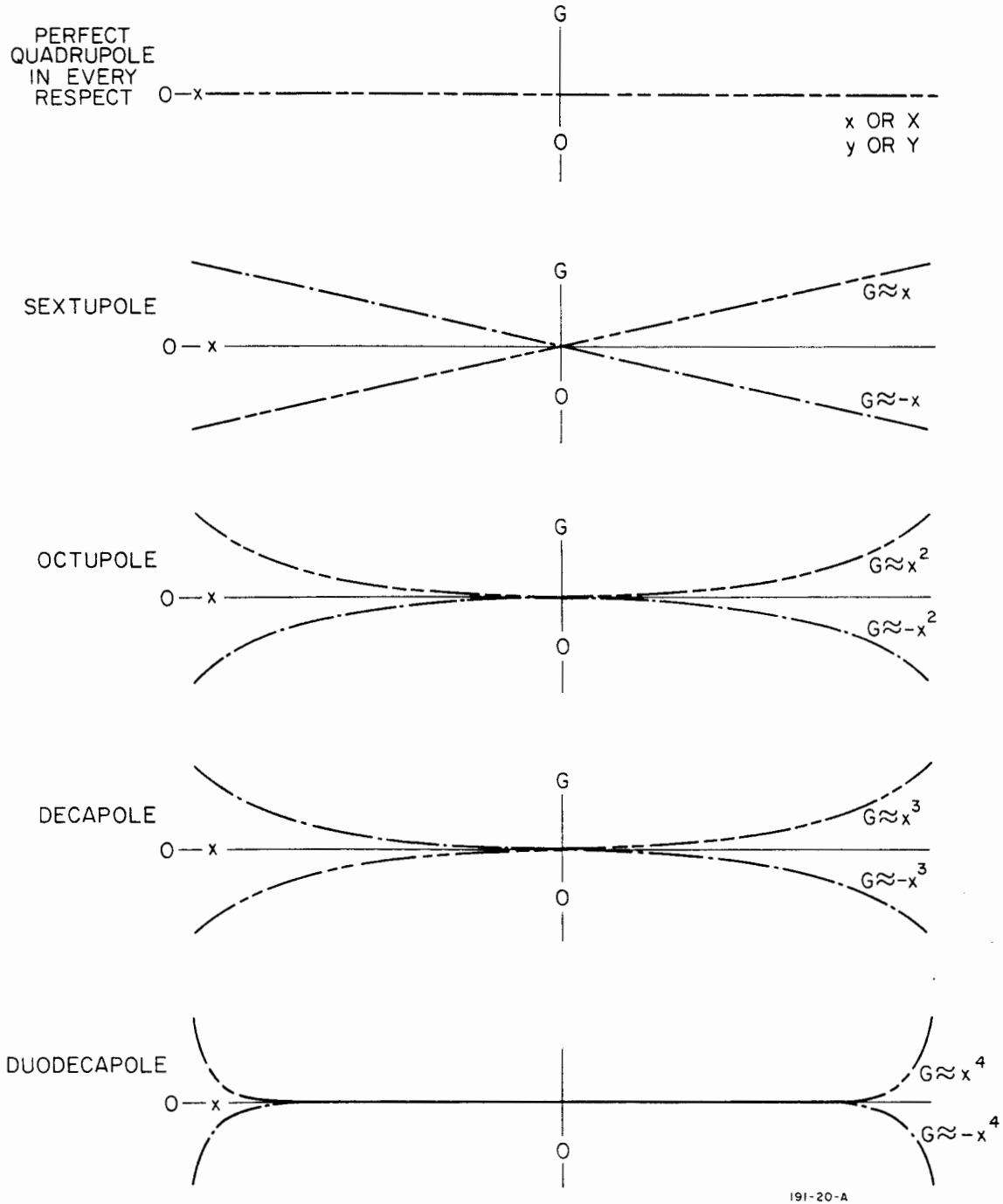


FIG. 30 - EFFECT OF VARIOUS MULTIPOLES ON THE GRADIENT VERSUS POSITION IN THE MAGNET APERTURE

where gradient G completely characterizes the field. Then, identifying the particle velocity v with \dot{z} , the time t can be eliminated from the motion equations with the relation $z = vt$, and we can write that

$$X'' - \frac{e}{p} B_Y = X'' - \frac{eG}{p} X = 0$$

and

$$Y'' + \frac{e}{p} B_X = Y'' + \frac{eG}{p} Y = 0$$

where $p = mv$ is the relativistic momentum of the particle.

When the quadrupole length ℓ_{eff} is so small that the deflection inside the quadrupole can be neglected (X, Y are constant in the magnet), the motion equations can be integrated directly

$$\Delta \left(\frac{dX}{dz} \right) = - \frac{eG\ell_{\text{eff}}}{p} X$$

$$\Delta \left(\frac{dY}{dz} \right) = + \frac{eG\ell_{\text{eff}}}{p} Y$$

In this approximation the quadrupole acts as a thin lens with the focal length

$$f = \frac{p}{eG\ell_{\text{eff}}} = \mp \frac{rB}{G\ell_{\text{eff}}}$$

that is, focusing in the XZ plane and defocusing in the YZ plane.

Introducing

$$K^2 = \frac{G}{rB}$$

and taking $z = 0$ at the entrance of the quadrupole, we can write the solution in a matrix form:

$$\begin{pmatrix} X \\ X' \end{pmatrix} = \begin{pmatrix} \cos Kl_{\text{eff}} & \frac{\sin Kl_{\text{eff}}}{K} \\ -K \sin Kl_{\text{eff}} & \cos Kl_{\text{eff}} \end{pmatrix} \begin{pmatrix} X_0 \\ X'_0 \end{pmatrix}$$

and

$$\begin{pmatrix} Y \\ Y' \end{pmatrix} = \begin{pmatrix} \cosh Kl_{\text{eff}} & \frac{\sinh Kl_{\text{eff}}}{K} \\ K \sinh Kl_{\text{eff}} & \cosh Kl_{\text{eff}} \end{pmatrix} \begin{pmatrix} Y_0 \\ Y'_0 \end{pmatrix}$$

Now the reciprocals of the focal lengths in the converging and diverging planes are given as

$$\frac{1}{f_c} = K \sin Kl_{\text{eff}} = K^2 l_{\text{eff}} \left(1 - \frac{1}{6} K^2 l_{\text{eff}}^2 + \dots \right)$$

$$\frac{1}{f_o} = -K \sinh Kl_{\text{eff}} = -K^2 l_{\text{eff}} \left(1 + \frac{1}{6} K^2 l_{\text{eff}}^2 + \dots \right)$$

It can be seen that the focusing properties of a quadrupole depend on the particle momentum. This effect, analogous to light optics where the location of the focal point depends on the light frequency, is called chromatic aberration. The chromatic aberration limits the momentum band that can be accepted if a given unsharpness of the image is not to be exceeded. The total apparent increase of the object size for a particle

with momentum $p + \Delta p$ is¹⁵

$$d = \frac{4}{\theta_0} \frac{\Delta p}{p} \frac{1}{2} \int_{p_0}^p (X')^2 dz$$

where θ_0 is the initial divergence and the trajectory is taken between points p_0 and p .

It was proposed¹⁶ that an achromatic quadrupole lens could be composed of two quadrupole lenses: an electrostatic lens and a magnetic lens. Figures 3la and 3lb show the achromatic quadrupole lenses with small and large apertures. The electrostatic field of the lens can be described by the scalar potential

$$\phi = \frac{E_0}{2} \left\{ f_1(z)(X^2 - Y^2) - \frac{1}{12} \frac{d^2 f_1(z)}{dz^2} (X^4 - Y^4) + \dots \right\}$$

and the magnetic field is given by the magnetic scalar potential as

$$u = H_0 \left\{ f_2(z)XY - \frac{1}{12} \frac{d^2 f_2(z)}{dz^2} XY(X^2 + Y^2) + \dots \right\}$$

When the two quadrupoles are not separated spacially and the electric and magnetic configurations are the same,

$$f_1(z) = f_2(z) = f(z)$$

and the motion equations can be written as

$$X'' - Xf(z) \left(\frac{eH_0}{mvc} - \frac{eE_0}{mv^2} \right) = 0$$

$$Y'' + Yf(z) \left(\frac{eH_0}{mvc} - \frac{eE_0}{mv^2} \right) = 0$$

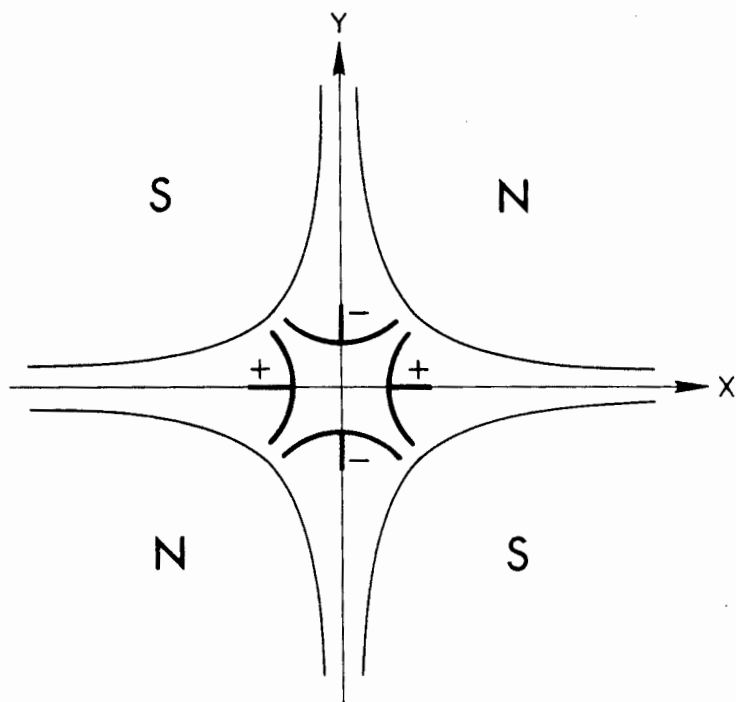
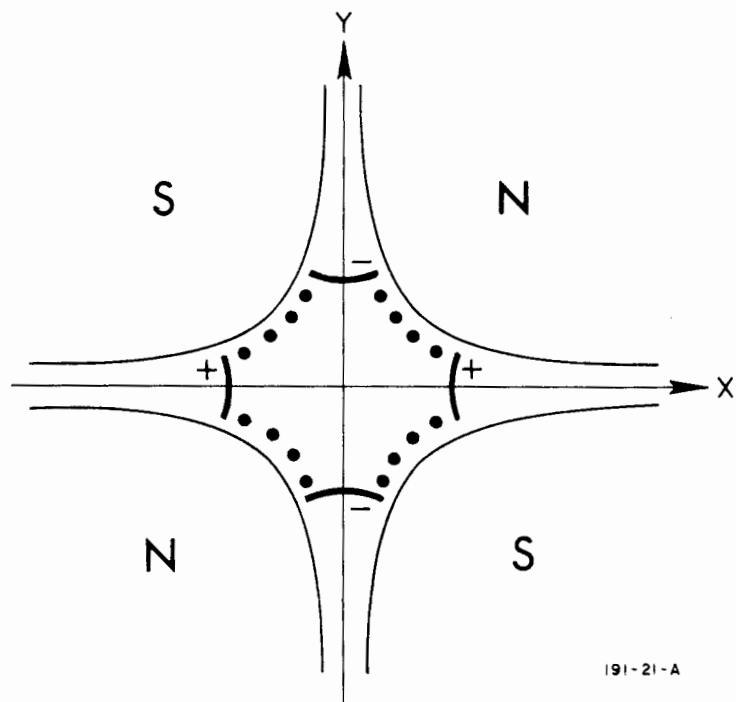


FIG. 31a - ACHROMATIC QUADRUPOLE LENS WITH POLES AND ELECTRODES OF HYPERBOLICAL FORM



191-21-A

FIG. 31b - ACHROMATIC QUADRUPOLE LENS WITH ENLARGED APERTURE

where v is the speed of the charged particle and the primes denote differentiation with respect to z . Introducing

$$Q(v) = \frac{eH_0}{mcv} - \frac{eE_0}{mv^2},$$

the requirement that the trajectory be independent of the speed of the particle is that $\left(\frac{dQ}{dv}\right)_{v=v_0} = 0$, which gives

$$E_0 = H_0 \frac{cv_0}{2c^2 - v_0^2}$$

and

$$Q = \frac{eE_0}{mv_0^2} \frac{c^2 - v_0^2}{c^2}$$

It has been shown that the chromatic aberration can be corrected in a quadrupole by using a sextupole magnet.^{17,18}

Similarly, for a sextupole field the magnetic scalar potential can be written as

$$u = \frac{B}{a^2} \left(X^2 Y - \frac{1}{3} Y^3 \right) = k \left(X^2 Y - \frac{1}{3} Y^3 \right)$$

where $k = \frac{B}{a^2}$ is the sextupole gradient. The magnetic field components B_X , B_Y may then be defined by

$$B_X = - \frac{\partial u}{\partial X} = -2kXY$$

$$B_Y = - \frac{\partial u}{\partial Y} = -k(X^2 - Y^2)$$

and with these, the motion equations can be written as

$$X'' + \frac{ek}{p} (X^2 - Y^2) = 0$$

$$Y'' - \frac{2ek}{p} XY = 0$$

These motion equations may be solved by numerical integration; however, simple approximate methods give good estimates in many practical cases.¹⁹

The motion equations in higher poles are even more complicated, and because of their infrequent use in transport systems, their optical properties are not well known. From this short discussion it is evident that for first-order optical calculations in quadrupoles, the effective length of the quadrupole field, the higher harmonic contents, and the gradients are needed as input data. From these and similar quantities for higher pole fields, the optical properties of the multipoles can be calculated.

ACKNOWLEDGEMENTS

The authors are most grateful to J. Ballam, H. Brechna, and R. Taylor of the Stanford Linear Accelerator Center for many helpful suggestions and to B. Hedin of CERN for valuable discussions.

LIST OF REFERENCES

1. E. D. Courant, M. S. Livingston, and H. S. Snyder, Phys. Rev. 91, 202 (1953).
2. E. D. Courant, M. S. Livingston, and H. S. Snyder, Phys. Rev. 88, 1190 (1952).
3. R. M. Johnson, Internal Report BeV-687, Lawrence Radiation Laboratory, Berkeley, California (1961).
4. J. J. Muray, submitted for publication to J. of Appl. Optics.
5. D. J. Craik and P. M. Griffiths, Proc. Phys. Soc. (Vol. B) 70, 1000 (1957).
6. D. J. Craik, Proc. Phys. Soc. (Vol. B) 69, 647 (1956).
7. H. C. van de Hulst, Light Scattering by Small Particles, (Wiley and Sons, New York, 1957).
8. J. K. Cobb and D. R. Jensen, Internal Report, Stanford Linear Accelerator Center, Stanford University, Stanford, California (1964).
9. M. G. Hine, CERN (P.S.) Int. MGNH Note 17, CERN, Geneva (1959) (unpublished).
10. J. J. Muray, Internal Report, Stanford Linear Accelerator Center, Stanford University, Stanford, California (1963).
11. W. C. Elmore and M. W. Garret, Rev. Sci. Instr. 25, 480 (1954).
12. I. E. Dayton, F. C. Shoemaker, and R. F. Mozley, Rev. Sci. Instr. 25, 485 (1954).
13. W. H. Lamb, Jr., WHL-1, Argonne National Laboratory (1962).
14. S. Penner, Rev. Sci. Instr. 32, 150 (1961).
15. B. de Raad, AR/Int. GS/62-5, CERN, Geneva (1962).
16. V. M. Kel'man and S. Ya. Yavor, Soviet Physics 6, No. 12, 1052 (1962).
17. S. van der Meer, CERN Report 60-22, CERN, Geneva (1960).
18. G. Chadwicks, CERN/TC/HBC-81, 62/22, CERN, Geneva (1962).
19. N. M. King, CERN Report MPS/EP-26, CERN, Geneva (1962).

LEGAL NOTICE

This report was prepared as an account of Government sponsored work. Neither the United States, nor the Commission, nor any person acting on behalf of the Commission:

A. Makes any warranty or representation, expressed or implied, with respect to the accuracy, completeness, or usefulness of the information contained in this report, or that the use of any information, apparatus, method, or process disclosed in this report may not infringe privately owned rights; or

B. Assumes any liabilities with respect to the use of, or for damages resulting from the use of any information, apparatus, method, or process disclosed in this report.

As used in the above, "person acting on behalf of the Commission" includes any employee or contractor of the Commission, or employee of such contractor, to the extent that such employee or contractor of the Commission, or employee of such contractor prepares, disseminates, or provides access to, any information pursuant to his employment or contract with the Commission, or his employment with such contractor.